NATIONAL TECHNICAL UNIVERSITY OF ATHENS
DEPARTMENT OF CIVIL ENGINEERING

**MSc Analysis and Design of Earthquake Resistant Structures
(ADERS)**

MASTER'S THESIS

Behaviour, Analysis and Design of
Steel Chimneys

PANAYIOTIS ANDREOU
BSc Civil and Environmental Engineer

Super visor: Charis J. Gantes, Associate Professor N.T.U.A

Athens, October 2011

NATIONAL TECHNICAL UNIVERSITY OF ATHENS
DEPARTMENT OF CIVIL ENGINEERING
DIVISION OF STRUCTURAL ENGINEERING
Laboratory of Steel Structures

Behaviour, Analysis and Design of Steel Chimneys

Master's Thesis
of Panayiotis Andreou

Supervisor: Charis J. Gantes, Associate Professor N.T.U.A.

Approved by three-member committee on the 17/10/2011:

J. Ioannidis, Professor,   ………………………..(Signature)

V. Koumousis, Professor,   …………………………..(Signature)

C. Gantes, Associate Professor,   ………………………….(Signature)

Athens, October 2011

PREFACE

The present master thesis titled o "Behaviour, Analysis and Design of Steel Chimneys" was conducted for the purposes of the interdisciplinary Postgraduate Studies Program "Analysis and Design of Earthquake Resistant Structures".

Initially, I need to express my gratitude to Mr. Charis Gantes, Associate Professor at the Department of Civil Engineering of N.T.U.A., for the assignment of this thesis and his support throughout its conduction. His excellent scientific specialization, combined with his endless willingness to help me in any way, were of significant importance for the completion of the present work.

I would also like to thank Mr. Petros Komodromos, Mr. Ioannis Mpalafas and Mr. Dimos Charmpis, Professors at the Department of Civil and Environmental Engineering of the University of Cyprus for motivating me in taking the specific postgraduate studies and their support during any difficulty I faced.

With this thesis, my presence in this program is reaching to its end. During this year, I made lots of friends and met worthy colleagues. I want to thank all my colleagues for the pleasant environment they created for me, their support and cooperation.

It would be a great omittance not to thank personally my friend and colleague Varnavas Varnava and my brother Andreas Andreou for the constant help and support they provided for until the completion of this work.

Also, I'd like to thank all my friends who, in their own way each one, encouraged and supported me during my studies.

Last, but not least, I ought to thank the people who are always by my side, in good and bad times, my parents Christodoulos and Chrysoula.

<div align="right">

Athens, October 2011

Panayiotis Andreou

</div>

"What doesn't kill me, makes me stronger"

NATIONAL TECHNICAL UNIVERSITY OF ATHENS
DEPARTMENT OF CIVIL ENGINEERING
DIVISION OF STRUCTURAL ENGINEERING
Laboratory of Steel Structures

Behaviour, Analysis and Design of Steel Chimneys

Master's Thesis
of Panayiotis Andreou

Supervisor: Charis J. Gantes, Associate Professor N.T.U.A.

Abstract

In this master's thesis the behaviour, analysis and design of steel chimneys is studied, using the final version of Eurocodes. Gases are passed through the chimney in the upper level of the atmosphere, mainly originating from industrial boilers. They are usually cylindrical, with height exceeding 40 m. In general, due to their dimensions, they are considered to be flexible constructions and as such they are prone to wind flow. Because of wind flow, the chimneys are also affected by vortex shedding. Then, the periodic alternately shedding of vortices leads to chimneys' oscillations transverse to the wind flow.

This work consists of ten chapters. The first chapter is a flashback to the chimneys' usage, construction materials, design methodologies and other important events that have contributed to the development of the current regulatory documents.

The second chapter presents the role of the chimneys to the environment. Reference is made to how geometry, operating conditions of the chimney and the state of the atmosphere affect the dispersal of pollutants exported from the chimney.

The third chapter refers to the design and construction methodologies of foundations of self-supported chimneys.

The fourth chapter presents the methodology for calculating the pressure and the total force acting to the chimney due to wind flow. The calculations are made according to EN1991-1-4. In the same

section, the criteria and the methodology for the check of the chimney against vortex shedding are presented. In the beginning of the chapter the background for understanding the behavior of chimneys under wind flow is cited.

The fifth chapter describes the process of analyzing the chimney under seismic loads, based on the EN1998-1.

In the sixth chapter the provisions of EN1991-1-5 for the calculation of thermal actions are provided.

The seventh chapter includes the provisions of EN1993-1-6 regarding the strength and stability of shells. It describes all possible methods of analysis and design of shells. It also presents the required checks for pertinent limit states: Plastic limit state (LSI), Cyclic plasticity limit state (LS2), Buckling limit state (LS3), Fatigue limit state (LS4) and also the serviceability limit state.

The eighth chapter presents the provisions of EN1993-3.2 on the design of steel chimneys. Also, information on methods of reducing the cross wind amplitude due to vortex shedding is provided. The methods concern the use of aerodynamic devices or dampers.

The ninth chapter presents an example of steel chimney. The example concerns the analysis and design of a steel chimney to be built in the framework of extension of the power station in the Greek island of Syros. The chimney is cylindrical with a constant outer diameter 3.753 m and height 60 m. The thickness of the chimney's shell is being reduced according to height. In this chapter all the loads imposed on the structure, i.e., self weight, wind loads (wind pressures and forces due to vortex shedding), seismic and thermal effects, are being calculated analytically. The chimney is modeled by using the finite elements software ADINA. For the purposes of the analysis two models are developed; model 1 by using shell finite elements; model 2 by using beam elements. Checks are performed for the four ultimate limit states (LS1, LS2, LS3 and LS4) as well as for the serviceability limit state. For every limit state all possible check methods are being developed, i.e., check based on membrane theory through the analytical functions of the Annex to EN1993-1-6, as well as with numerical non linear analyses. For each analysis there is presentation and discussion of the results produced from every applied method. Additionally, the checks are carried out for both model 1 and model 2. At the ultimate limit state LS4 the reduction of the maximum width and model of transverse oscillation is being examined through aerodynamic devices and with the use of a damper.

Finally, the tenth chapter presents general conclusions about the behaviour, analysis and design of steel chimneys, as they have emerged from the present study. Furthermore, it proposes ad hoc suggestions for future studies on issues that need further investigation.

CONTENTS

FIGURES' CONTENTS

TABLES' CONTENTS

<div align="right">

1
INTRODUCTION

</div>

This thesis presents the analysis process and design of a steel chimney in accordance with Eurocodes. The example concerns the analysis study and design of a chimney which will be erected during the construction of a DEH independent power plant (APS) of the greek electricity association in Syros. The finite element software ADINA which can perform non-linear analysis was used for the analysis purposes. Initially, are presented the assumptions used for modeling, ie. geometry, support conditions and loading calculations. Follows the simulation methodology at the particular software package and finally are presented the results of the analysis. For the modeling, are used two static simulants, a bar model and a spatial model of finite shell elements. Also, is noted that all the available methods of failure controlling are developed (through stress, numerical analysis), combining linearity and non-linearity of a material and its geometry. In the end of each analysis are presented the results obtained by all methods and comparative reviews.

1.1. Description of the chimney

The chimney which will be constructed in IEP of Syros is mutineer double skin type, outer diameter 3.735m and height 60m. It is made of steel CORTEN S355-A. It has three internal flues (lumens) with

an internal diameter 1000 mm, 1273 mm and 1130 mm which carry the exhaust of one chimney CEGIELSKI, two units GMT-FIAT with power 5.85 MW and two units GMT-FIAT with power 3.5 MW, respectively.

The flues are complete continuous welded to achieve solidarity. Every chimney is insulated with mineral wool of density 100kg/m^3 and thickness 100mm. The isolation protection is achieved with an aluminium foil of thickness 1mm which is held by rings every 1m.

The chimney consists of 5 individual pieces of cylindrical shells of different thickness and height but constant outer diameter. The corresponding dimensions are indicated in *Figure 1.1*.

The chimney will be assembled on site using the appropriate screw connections.
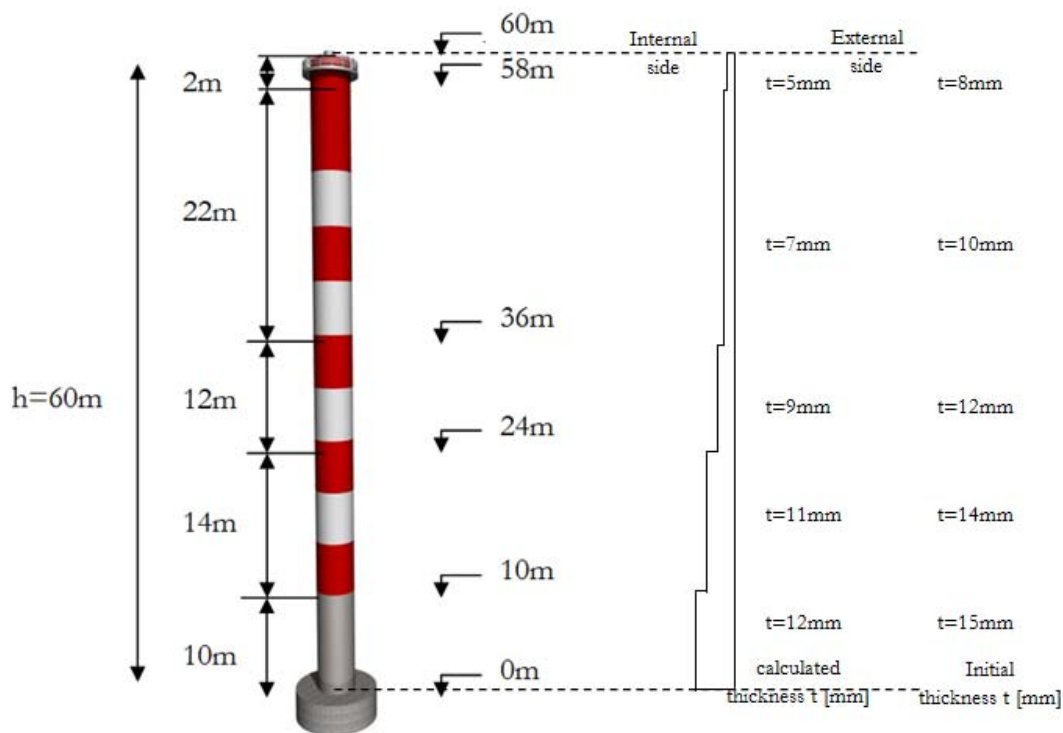
Figure 1.1: An outline of the chimney

1.2. Modelling of geometry

The chimney consists of a vertical, cylindrical steel bearer of 60m heigh. The thickness of the chimney's shell isr educed vertically. Different thicknesses are used for economic reasons as is shown in *Figure 1.1.* The chimney consists of 5 individual cylindrical shells parts each with constant thickness that will be assembled together by screw connections. It is assumed that the links will take

capacity design study to prevent collapse before the shell failure. In place of compounds diaphragmatic operation is defined. On the construction of body's shell, should be take into account the reduction of the intersection due to corrosion. For the specific chimney is assumed that a regular maintenance with paint will be done (in 1mm/year). Therefore, in the analysis is considered that the total reduction of intersection is 3mm. In **Table 1. 1** is shown the intersection's thickness in height, before and after the corrosion. For modeling reason, is assumed that the model diameter remains constant (3.735mm) and only the thickness is changes.

Table 1. 1: Initial and reduced thickness of the structure vertically

Part	Length (m)	Total Length (m)	Initial Thickness (mm)	Reduced Thickness (mm)	Internal Model Diameter (mm)
1	10.00	10.00	15	12	3723
2	14.00	24.00	14	11	3724
3	12.00	36.00	12	9	3726
4	22.00	58.00	10	7	3728
5	2.00	60.00	8	5	3730

1.2.1. *Support conditions*

The construction is grounded on circular section bored piles. There will not be equipped with cables racing. Therefore, on the body base are considered support conditions, full-anchorage for transport movements. Rotational freedom around axes X and Y is considered.

1.2.2. *Material*

Steel CORTEN S355 is the material used for all models. In **Table 1. 2** and **1.3.** are shown the mechanical properties of the material at temperatures 25° C and 50° C, respectively. It is assumed that during the operation of the chimney, the shell body will be exposed to temperatures up to 50° C. Consecuently for the purpose of analysis the reduced mechanical properties of steel for temperature 50° C are considered.

Table 1. 2: Mechanical properties of steel CORTEN S355 at temperature 25º C

Mechanical Properties	Symbol	Price	Measurment Units
Elasticity Module	E	199.00	GPA
Poisson Ratio	ν	0.33	-
Density	ρ	7850.00	Kg/m^3
Yield in capacity	fy	355.00	MPa
Ultimate capacity	fu	470	MPa

Table 1. 3: Mechanical properties of steel CORTEN S355 at temperature 50º C

Mechanical properties	Symbol	Price	Measurment Units
Elasticity Module	E	170.00	GPA
Poisson Ratio	ν	0.33	-
Density	ρ	7850.00	Kg/m^3
Yield Capacity	fy	345.00	MPa
Ultimate Capacity	fu	-	MPa
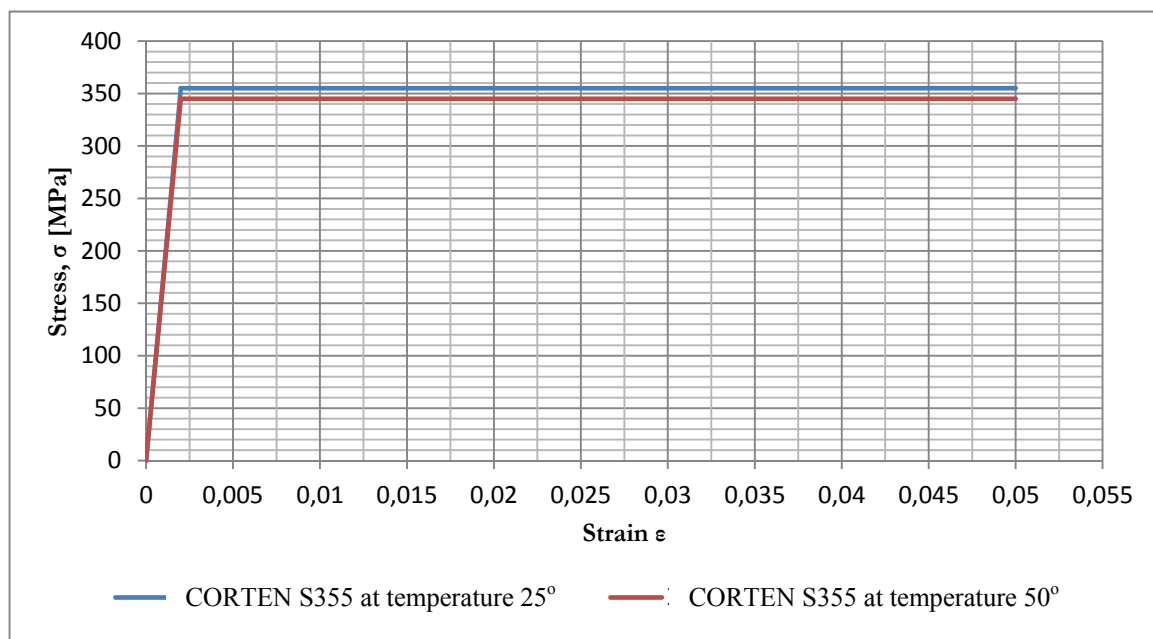
Figure 1.2: Stress-strain diagram

The chimney will be analyzed assuming linearity and non-linearity of the material. At the first case, the material has the properties which are shown at the above tables. In the non-linearity scenario the behavior of the material will described by a bi-linear stress strain model, as shown in

2

CALCULATION OF THE LOADS

2.1. Self weight loads

As the permanent loads of the chimney is considered to have itself weight of the shelled body (without the influence of the corrosion) and the same weight of non-bearing elements as investments, insulations, flues e.t.c. The shelf weight of the shelled-body is taken into account. It can be determined from the formula:

$$Ws = 2 \cdot G \cdot \pi \cdot r \cdot \sum_{i=1}^{5} t_i \cdot l_i$$

where:

G   the shelf weight of steel construction

r   the outer radius of the chimney

t_i, l_i the thickness and the length, respectively, of section i

Therefore:

$$Ws = 2G \cdot \pi \cdot r(15mm \cdot 10 + 14mm \cdot 14m + 12mm \cdot 12m + 10mm \cdot 22m + 8mm \cdot 2m = 668.724kN$$

For the example purposes, it has not taken into account every additional coating weight or the Liners' weight, thus:

$$Wa = 0 kN$$

Consecuently, the total weight of the chimney is:

$$Wt = Ws + Wa = 668.724 kN$$

The ratio between supporting structure and the total weight is:

$$\frac{Ws}{Wt} = 1$$

2.2. Wind loads

2.2.1. *Calculate the wind pressure*

The total wind pressure which acts vertically at the outer structure surface, as the chimneys can be calculated by the following formula:

$$w_e = q_p(z_e) \cdot c_{pe}$$

The calculation of the factors of the previous equation are based on the provisions of EN1991-1-4.For the particular example the assumes which are described below are valued.

The chimney is designed for wind velocity 200km/h (=55.6 m/s) instead of 33 km/h which is proposed in the EN1991-1-4 for islands. Therefore, the basic wind velocity is:

$$v_b = 55.6 m/s \cdot 1 \cdot 1 = 55.6 m/s$$

The construction area of the chimney is considered class III. As it can be seen from ***Table 2.1 – 2.6*** the values of Re number is class x10^7. Consequently are valid the following values:

- α_{min} the position of the minimum pressure = 75°
- $\alpha_{p0,min}$ the magnitude of the minimum pressure coefficient = 1.5
- α_A the position of the flow separation = 105°
- $\alpha_{p0,h}$ the coefficient of the basic pressure

For the shell of the chimney is assumed equivalent rough k=0.05. Therefore, considering that:

$$\frac{k}{b} = 1.339 \cdot 10^{-5} < 5 \cdot 10^{-4}$$

The coefficient's $c_{p,0}$ values can be taken from the ***Figure 7.27*** (EN1991-1-4).

In order to calculate the final wind pressure, the outer pressures should be multiplied with the dynamic coefficient, so that this way the dynamic behavior of the wind will be taken into account. The calculation of the dynamic factor is presented on the next paragraph.

All the calculations to determine the outer wind pressure on discrete points at vertically on the chimney, are presented at *Table 2.1. – 2.6.*

Table 2.1: Calculate wind pressure, reference height 5m

z=	5
c_{rz}=	0,61
c_{0z}=	1,00
kI=	1,00
c_0=	1,00

Angle (°)	[v_m]	[I_{vz}]	[$q_{p(z)}$] kN/m²	[v_{ze}] m/s	Re	α_{min} (°)	α_A (°)	[c_{p0}]	ψ_λ	$\psi\lambda\alpha$	[c_{pe}]	[w] kN/m²
0	33,692	0,355	2,475	62,925	1,567E+07	75	105	1,000	0,730	1,000	1,000	2,475
10	33,692	0,355	2,475	62,925	1,567E+07	75	105	0,850	0,730	1,000	0,850	2,104
20	33,692	0,355	2,475	62,925	1,567E+07	75	105	0,400	0,730	1,000	0,400	0,990
31	33,692	0,355	2,475	62,925	1,567E+07	75	105	0,000	0,730	1,000	0,000	0,000
40	33,692	0,355	2,475	62,925	1,567E+07	75	105	-0,300	0,730	1,000	-0,300	-0,742
55	33,692	0,355	2,475	62,925	1,567E+07	75	105	-0,500	0,730	1,000	-0,500	-1,237
60	33,692	0,355	2,475	62,925	1,567E+07	75	105	-1,250	0,730	1,000	-1,250	-3,093
75	33,692	0,355	2,475	62,925	1,567E+07	75	105	-1,500	0,730	1,000	-1,500	-3,712
80	33,692	0,355	2,475	62,925	1,567E+07	75	105	-1,500	0,730	0,991	-1,486	-3,678
90	33,692	0,355	2,475	62,925	1,567E+07	75	105	-1,350	0,730	0,921	-1,243	-3,077
100	33,692	0,355	2,475	62,925	1,567E+07	75	105	-1,350	0,730	0,800	-1,080	-2,672
105	33,692	0,355	2,475	62,925	1,567E+07	75	105	-0,800	0,730	0,730	-0,584	-1,445
180	33,692	0,355	2,475	62,925	1,567E+07	75	105	-0,800	0,730	0,730	-0,584	-1,445

Table 2.2: Calculate wind pressure, reference height 10m

z=	10
c_{rz}=	0,76
c_{0z}=	1,00
kI=	1,00
c_0=	1,00

Angle (°)	[v_m]	[I_{vz}]	[$q_{p(z)}$] kN/m²	[v_{ze}] m/s	Re	α_{min} (°)	α_A (°)	[c_{p0}]	ψ_λ	$\psi\lambda\alpha$	[c_{pe}]	[w] kN/m²
0	41,993	0,285	3,302	72,689	1,810E+07	75	105	1,000	0,730	1,000	1,000	3,302
10	41,993	0,285	3,302	72,689	1,810E+07	75	105	0,850	0,730	1,000	0,850	2,807
20	41,993	0,285	3,302	72,689	1,810E+07	75	105	0,400	0,730	1,000	0,400	1,321
31	41,993	0,285	3,302	72,689	1,810E+07	75	105	0,000	0,730	1,000	0,000	0,000
40	41,993	0,285	3,302	72,689	1,810E+07	75	105	-0,300	0,730	1,000	-0,300	-0,991
55	41,993	0,285	3,302	72,689	1,810E+07	75	105	-0,500	0,730	1,000	-0,500	-1,651
60	41,993	0,285	3,302	72,689	1,810E+07	75	105	-1,250	0,730	1,000	-1,250	-4,128
75	41,993	0,285	3,302	72,689	1,810E+07	75	105	-1,500	0,730	1,000	-1,500	-4,953
80	41,993	0,285	3,302	72,689	1,810E+07	75	105	-1,500	0,730	0,991	-1,486	-4,908
90	41,993	0,285	3,302	72,689	1,810E+07	75	105	-1,350	0,730	0,921	-1,243	-4,106
100	41,993	0,285	3,302	72,689	1,810E+07	75	105	-1,350	0,730	0,800	-1,080	-3,566
105	41,993	0,285	3,302	72,689	1,810E+07	75	105	-0,800	0,730	0,730	-0,584	-1,929
180	41,993	0,285	3,302	72,689	1,810E+07	75	105	-0,800	0,730	0,730	-0,584	-1,929

Table 2.3: Calculate wind pressure, reference height 24m

$z=$	24
$c_{rz}=$	0,94
$c_{0z}=$	1,00
$kI=$	1,00
$c_0=$	1,00

Angle (^{o})	$[v_m]$	$[I_{vz}]$	$[q_{p(z)}]$ kN/m^2	$[v_{ze}]$ m/s	Re	α_{min} (^{o})	α_A (^{o})	$[c_{p0}]$	ψ_λ	$\psi\lambda\alpha$	$[c_{pe}]$	$[w]$ kN/m^2
0	52,478	0,228	4,471	84,576	2,106E+07	75	105	1,000	0,730	1,000	1,000	4,471
10	52,478	0,228	4,471	84,576	2,106E+07	75	105	0,850	0,730	1,000	0,850	3,800
20	52,478	0,228	4,471	84,576	2,106E+07	75	105	0,400	0,730	1,000	0,400	1,788
31	52,478	0,228	4,471	84,576	2,106E+07	75	105	0,000	0,730	1,000	0,000	0,000
40	52,478	0,228	4,471	84,576	2,106E+07	75	105	-0,300	0,730	1,000	-0,300	-1,341
55	52,478	0,228	4,471	84,576	2,106E+07	75	105	-0,500	0,730	1,000	-0,500	-2,235
60	52,478	0,228	4,471	84,576	2,106E+07	75	105	-1,250	0,730	1,000	-1,250	-5,588
75	52,478	0,228	4,471	84,576	2,106E+07	75	105	-1,500	0,730	1,000	-1,500	-6,706
80	52,478	0,228	4,471	84,576	2,106E+07	75	105	-1,500	0,730	0,991	-1,486	-6,644
90	52,478	0,228	4,471	84,576	2,106E+07	75	105	-1,350	0,730	0,921	-1,243	-5,558
100	52,478	0,228	4,471	84,576	2,106E+07	75	105	-1,350	0,730	0,800	-1,080	-4,828
105	52,478	0,228	4,471	84,576	2,106E+07	75	105	-0,800	0,730	0,730	-0,584	-2,611
180	52,478	0,228	4,471	84,576	2,106E+07	75	105	-0,800	0,730	0,730	-0,584	-2,611

Table 2.4: Calculate wind pressure, reference height 36m

z=	36
c_{rz}=	1,03
c_{0z}=	1,00
kI=	1,00
c_0=	1,00

Angle (°)	$[v_m]$	$[I_{vz}]$	$[q_{p(z)}]$ kN/m²	$[v_{ze}]$ m/s	Re	α_{min} (°)	α_A (°)	$[c_{p0}]$	ψ_λ	$\psi\lambda\alpha$	$[c_{pe}]$	$[w]$ kN/m²
0	57,333	0,209	5,058	89,963	2,240E+07	75	105	1,000	0,730	1,000	1,000	5,058
10	57,333	0,209	5,058	89,963	2,240E+07	75	105	0,850	0,730	1,000	0,850	4,300
20	57,333	0,209	5,058	89,963	2,240E+07	75	105	0,400	0,730	1,000	0,400	2,023
31	57,333	0,209	5,058	89,963	2,240E+07	75	105	0,000	0,730	1,000	0,000	0,000
40	57,333	0,209	5,058	89,963	2,240E+07	75	105	-0,300	0,730	1,000	-0,300	-1,517
55	57,333	0,209	5,058	89,963	2,240E+07	75	105	-0,500	0,730	1,000	-0,500	-2,529
60	57,333	0,209	5,058	89,963	2,240E+07	75	105	-1,250	0,730	1,000	-1,250	-6,323
75	57,333	0,209	5,058	89,963	2,240E+07	75	105	-1,500	0,730	1,000	-1,500	-7,587
80	57,333	0,209	5,058	89,963	2,240E+07	75	105	-1,500	0,730	0,991	-1,486	-7,518
90	57,333	0,209	5,058	89,963	2,240E+07	75	105	-1,350	0,730	0,921	-1,243	-6,289
100	57,333	0,209	5,058	89,963	2,240E+07	75	105	-1,350	0,730	0,800	-1,080	-5,462
105	57,333	0,209	5,058	89,963	2,240E+07	75	105	-0,800	0,730	0,730	-0,584	-2,954
180	57,333	0,209	5,058	89,963	2,240E+07	75	105	-0,800	0,730	0,730	-0,584	-2,954

Table 2.5: Calculate wind pressure, reference height 58m

$z=$ 58

$c_{rz}=$ 1,13

$c_{0z}=$ 1,00

$kI=$ 1,00

$c_0=$ 1,00

Angle (°)	$[v_m]$	$[I_{vz}]$	$[q_{p(z)}]$ kN/m²	$[v_{ze}]$ m/s	Re	α_{min} (°)	α_A (°)	$[c_{p0}]$	ψ_λ	$\psi_\lambda\alpha$	$[c_{pe}]$	$[w]$ kN/m²
0	63,045	0,190	5,787	96,227	2,396E+07	75	105	1,000	0,730	1,000	1,000	5,787
10	63,045	0,190	5,787	96,227	2,396E+07	75	105	0,850	0,730	1,000	0,850	4,919
20	63,045	0,190	5,787	96,227	2,396E+07	75	105	0,400	0,730	1,000	0,400	2,315
31	63,045	0,190	5,787	96,227	2,396E+07	75	105	0,000	0,730	1,000	0,000	0,000
40	63,045	0,190	5,787	96,227	2,396E+07	75	105	-0,300	0,730	1,000	-0,300	-1,736
55	63,045	0,190	5,787	96,227	2,396E+07	75	105	-0,500	0,730	1,000	-0,500	-2,894
60	63,045	0,190	5,787	96,227	2,396E+07	75	105	-1,250	0,730	1,000	-1,250	-7,234
75	63,045	0,190	5,787	96,227	2,396E+07	75	105	-1,500	0,730	1,000	-1,500	-8,681
80	63,045	0,190	5,787	96,227	2,396E+07	75	105	-1,500	0,730	0,991	-1,486	-8,601
90	63,045	0,190	5,787	96,227	2,396E+07	75	105	-1,350	0,730	0,921	-1,243	-7,195
100	63,045	0,190	5,787	96,227	2,396E+07	75	105	-1,350	0,730	0,800	-1,080	-6,249
105	63,045	0,190	5,787	96,227	2,396E+07	75	105	-0,800	0,730	0,730	-0,584	-3,380
180	63,045	0,190	5,787	96,227	2,396E+07	75	105	-0,800	0,730	0,730	-0,584	-3,380

Table 2.6: Calculate wind pressure, reference height 60m

z=	60
c_{rz}=	1,14
c_{0z}=	1,00
kI=	1,00
c_0=	1,00

Angle (°)	$[v_m]$	$[I_{vz}]$	$[q_{p(z)}]$ kN/m^2	$[v_{ze}]$ m/s	Re	α_{min} (°)	α_A (°)	$[c_{p0}]$	ψ_λ	$\psi\lambda\alpha$	$[c_{pe}]$	$[w]$ kN/m^2
0	63,451	0,189	5,841	96,670	2,407E+07	75	105	1,000	0,730	1,000	1,000	5,841
10	63,451	0,189	5,841	96,670	2,407E+07	75	105	0,850	0,730	1,000	0,850	4,965
20	63,451	0,189	5,841	96,670	2,407E+07	75	105	0,400	0,730	1,000	0,400	2,336
31	63,451	0,189	5,841	96,670	2,407E+07	75	105	0,000	0,730	1,000	0,000	0,000
40	63,451	0,189	5,841	96,670	2,407E+07	75	105	-0,300	0,730	1,000	-0,300	-1,752
55	63,451	0,189	5,841	96,670	2,407E+07	75	105	-0,500	0,730	1,000	-0,500	-2,920
60	63,451	0,189	5,841	96,670	2,407E+07	75	105	-1,250	0,730	1,000	-1,250	-7,301
75	63,451	0,189	5,841	96,670	2,407E+07	75	105	-1,500	0,730	1,000	-1,500	-8,761
80	63,451	0,189	5,841	96,670	2,407E+07	75	105	-1,500	0,730	0,991	-1,486	-8,680
90	63,451	0,189	5,841	96,670	2,407E+07	75	105	-1,350	0,730	0,921	-1,243	-7,261
100	63,451	0,189	5,841	96,670	2,407E+07	75	105	-1,350	0,730	0,800	-1,080	-6,307
105	63,451	0,189	5,841	96,670	2,407E+07	75	105	-0,800	0,730	0,730	-0,584	-3,411
180	63,451	0,189	5,841	96,670	2,407E+07	75	105	-0,800	0,730	0,730	-0,584	-3,411

2.2.2.   Calculate the wind force

EN1991-4 allows the calculation of the total wind power (power per meter) instead of the allocation of the wind pressure at the outers of the chimney. This method is approximated and usually is appropriate in the static simulation with ribbed elements case analysis. The total wind power is provided from the following formula:

$$F_w = c_s c_d \cdot c_f \cdot q_p(z_e) \cdot A$$

c_f and $q_p(z_e)$ coefficients are calculated with the relationships proposed by EN1991-1-4. Thereafter, the calcul.ation of the dynamic factor $c_s c_d$ follows. This calculation can be made with detailed procedures (Annex B and C of EN1991-1-4) or the approximate method. For the calculation of the coefficients the determination of the constructive logarithmic dumping is required

The foundamental logarithmic structure percentage of the decreasing dumping is shown at **Table F2** (EC1). For welded steel chimneys with a layer of lining and an outer thermal isulation is:

$$\delta s = 0.020 \text{ for h/b<18m}$$

Because the dynamic coefficient is estimated from **Figure F.D.1** and takes values greater than 1.1, should be calculated using the analytical method. At the Annex B and C of EN 1991-1-4 are respectively proposed two analytical methods for the calculation of the dynamic coefficient. In the present study for the comparison purposes, the dynamic coefficient is calculated using both methods.

The structure coefficient $c_s c_d$ may be calculated using the formula:

$$c_s c_d = \frac{1 + 2 \cdot k_p \cdot I_v(z_e) \cdot \sqrt{B^2 + R^2}}{1 + 7 \cdot I_v(z_e)}$$

z_e is the reference height

k_p is the peak coefficient defined as the ratio of the maximum value of the fluctuating part of the response to its standard deviation

I_v is the turbulence intensity

B^2 is the background coefficient, allowing for the lack of full correlation of the pressure on the structure surface

R^2 is the resonance response coefficient, allowing for turbulence in resonance with the vibration mode.

- ***Procedure 1 for determining the structural coefficient $c_s c_d$***

The background coefficient B^2 allowing for the lack of full correlation of the pressure on the structure surface may be calculated using Formula:

$$B^2 = \frac{1}{1 + 0.9 \cdot \left(\dfrac{b+h}{L(z_e)}\right)^{0.63}}$$

Where:

b= 3.735m   is the width of the structure..

h= 60m   is the height of the structure

$L(z_e)$ is the turbulent length scale at reference height z_e .

The turbulent length scale $L(z)$ represents the average gust size for natural winds. For heights z below 200 m the turbulent length scale may be calculated using formula:

$$L(z) = L_t \cdot \left(\frac{z}{z_t}\right)^a \quad \text{for } z > z_{\min}$$

$$L(z) = L(z_{\min}) \quad \text{for } z < z_{\min}$$

with a reference height of z_t = 200 m, a reference length scale of L_t = 300 m, and with a=0.67+0.05ln(z_0), where the roughness length $z0$ is in m.

The EN1991-4 gives you the opportunity to take protective B2 equal to 1.
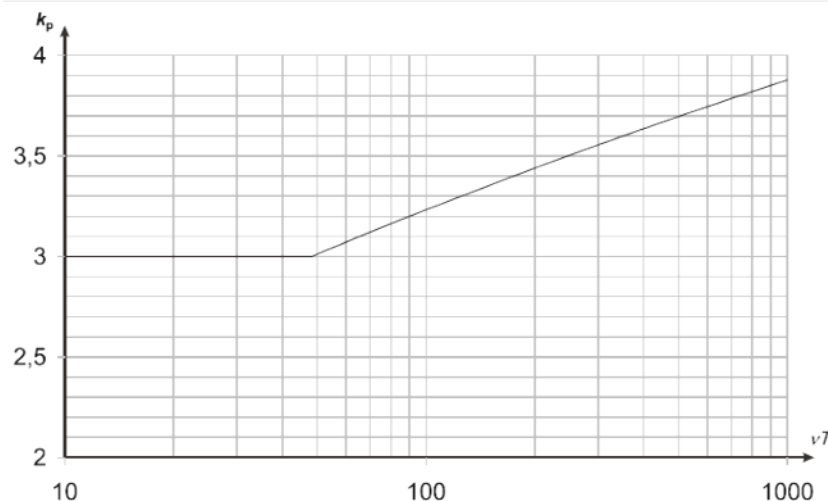

Figure 2. 1:Peak coefficient kp

The peak coefficient k_p, defined as the ratio of the maximum value of the fluctuating part of the response to its standard deviation, should be obtained from Formula:

$$k_p = \max \begin{cases} \sqrt{2 \cdot \ln(v \cdot T)} + \dfrac{0.6}{\sqrt{2 \cdot \ln(v \cdot T)}} \\ 3 \end{cases}$$

and is shown in

Figure 2. 1.

where:

T   is the averaging time for the mean wind velocity, $T = 600$ seconds

v is the up-crossing frequency given from:

$$v = n_{1,x} \sqrt{\frac{R^2}{B^2 + R^2}} \quad v > 0.08 \text{ Hz}$$

Where $n_{1,x}$ is the natural frequency of the structure.

The resonance response coefficient R^2, allowing for turbulence in resonance with the considered vibration mode of the structure should be determined using Formula:

$$R^2 = \frac{\pi^2}{2 \cdot \delta} \cdot S_L(z_e, n_{1,x}) \cdot R_h(\eta_h) \cdot R_b(\eta_b)$$

where:

δ is the total logarithmic decrement of damping

S_L is the non-dimensional power spectral density function given from:

$$S_L(z, n) = \frac{6.8 \cdot f_L(z, n)}{(1 + 10.2 \cdot f_L(z, n))^{5/3}}$$

where $f_L(z, n) = \dfrac{n \cdot L(z)}{v_m(z)}$ is a non-dimensional frequency determined by the frequency $n = n_{1,x}$, the natural frequency of the structure in Hz, by the mean velocity $v_m(z)$ and the turbulence length scale $L(z)$.

R_h, R_b is the aerodynamic admittance functions given as:

$$R_h = \frac{1}{\eta_h} - \frac{1}{2 \cdot \eta_h^2}(1 - e^{-2 \cdot \eta_h}) \qquad R_h = 1 \text{ for } \eta_h = 0$$

$$R_b = \frac{1}{\eta_b} - \frac{1}{2 \cdot \eta_b^2}(1 - e^{-2 \cdot \eta_b}) \qquad R_b = 1 \text{ for } \eta_b = 0$$

with: $\qquad \eta_h = \frac{4.6 \cdot h}{L(ze)} \cdot f_L(z_e, n_{1,x}) \qquad$ and $\qquad \eta_b = \frac{4.6 \cdot b}{L(ze)} \cdot f_L(z_e, n_{1,x})$

then calculate the structural coefficient $c_s c_d$ for this example.

For terrain category III is:

$$z_0 = 0.3m \text{ and } z_{min} = 5m$$

for the chimney is:

$$b = 3.735m, \text{ diameter.}$$

$$h = 60m, \text{ height.}$$

So the turbulent length is:

$$L(z) = L_t \cdot \left(\frac{z}{z_t}\right)^a = 300 \cdot \left(\frac{36}{200}\right)^{0.61} = 105.435m$$

where:

a=0.67+0.05 ln(0.3)=0.61

zt =200m, Lt=300m and z=0.6·h=36m

the roughness coefficient and the maximum average wind obtained from previous calculations, for reference height 36m.:

$$c_r(z) = 0.921$$

$$v_m(z) = 51.213m/s$$

The background coefficient B2 is:

$$B^2 = \frac{1}{1 + 0.9 \cdot \left(\frac{b+h}{L(z_e)}\right)^{0.63}} = \frac{1}{1 + 0.9 \cdot \left(\frac{3.735m + 60m}{105.435m}\right)^{0.63}} = 0.604$$

the fundamental flexural frequency of structure is:

$$n_1 = \frac{\varepsilon_1 \cdot b}{h_{eff}^2} \cdot \sqrt{\frac{W_s}{W_t}} [Hz] \text{ (F.3)}$$

$$\mu\varepsilon \quad h_{eff} = h_1 + \frac{h_2}{3} \text{ (F.4)}$$

where:

b   is the top diameter of the chimney [m]

h_{eff} is the effective height of the chimney [m], h_1 and h_2 are given in Figure F.1,(EN1991-1-4)

W_s is the weight of structural parts contributing to the stiffness of the chimney,

W_t is the total weight of the chimney

ε_1 is equal to 1000 for steel chimneys, and 700 for concrete and masonry chimneys.

For this chimney, h_2=0. So:

$$h_{eff} = h_1 = h = 60m$$

Based on the above, suggests:

$$n_1 = \frac{1000 \cdot 3.735}{60^2} \cdot \sqrt{1} = 1.038 [Hz]$$

and:

$$f_L(z,n) = \frac{n \cdot L(z)}{v_m(z)} = \frac{1.038 Hz \cdot 105.435 m}{51.213 m/s} = 2.137$$

and:

$$S_L(z,n) = \frac{6.8 \cdot f_L(z,n)}{(1+10.2 \cdot f_L(z,n))^{5/3}} \frac{6.8 \cdot 2.137}{(1+10.2 \cdot 2.137)^{5/3}} = 0.079$$

additional:

$$\eta_h = \frac{4.6 \cdot h}{L(ze)} \cdot f_L(z_e, n_{1,x}) = \frac{4.6 \cdot 60m}{105.435m} \cdot 2.137 = 5.594$$

$$\eta_b = \frac{4.6 \cdot b}{L(ze)} \cdot f_L(z_e, n_{1,x}) = \frac{4.6 \cdot 3.735m}{105.435} \cdot 2.137 = 0.348$$

The aerodynamic admittance functions for a fundamental mode shape may be approximated using Formulas:

$$R_h = \frac{1}{\eta_h} - \frac{1}{2 \cdot \eta_h^2}(1-e^{-2 \cdot \eta_h}) = \frac{1}{5.594} - \frac{1}{2 \cdot 5.594^2}(1-e^{-2 \cdot 5.594}) = 0.163$$

$$R_b = \frac{1}{\eta_b} - \frac{1}{2 \cdot \eta_b^2}(1-e^{-2 \cdot \eta_b}) = \frac{1}{0.348} - \frac{1}{2 \cdot 0.348^2}(1-e^{-2 \cdot 0.348}) = 0.803$$

the total logarithmic decrement of damping for the bending fundamental frequency is:

$$\delta = \delta_s + \delta_a + \delta_d$$

where δs=0.02 resulting from previous calculations.

the logarithmic decrement of damping δ_a for bending fundamental frequency modal accros the wind can be calculated with formula:

$$\delta_a = \frac{c_f \cdot \rho \cdot v_m(z_e)}{2 \cdot n_1 \cdot \mu_e} \quad (4.\,1)$$

where:

$$c_f = c_{f,0} \cdot \psi_\lambda$$

ψ_λ=0. resulting from previous calculations and

$$cf_0 = 1.2 + \frac{0.18 \cdot \log(10 \cdot k / b)}{1 + 0.4 \cdot \log(\mathrm{Re}/10^6)} = 1.2 + \frac{0.18 \cdot \log(10 \cdot 0.05mm / 3.735m)}{1 + 0.4 \cdot \log(2.00x10^7 / 10^6)} = 0.741$$

So:

$$c_f = 0.741 \cdot 0.73 = 0.541$$

μ_c: is the equivalent mass per unit area of the structure which for rectangular areas. Approximately calculated as:

$$\mu_e = \frac{Ws}{h} = \frac{668.724kN}{60m} = 11.145kN / m$$

Then:

$$\delta_a = \frac{0.546 \cdot 0.0125kN / m^3 \cdot 57.333m / s}{2 \cdot 1.038Hz \cdot 11.145kN / m} = 0.063$$

And:

$$\delta = 0.02 + 0.063 + 0 = 0.083$$

So, the resonance response coefficient is:

$$R^2 = \frac{\pi^2}{2 \cdot \delta} \cdot S_L(z_e, n_{1,x}) \cdot R_h(\eta_h) \cdot R_b(\eta_b) = \frac{\pi^2}{2 \cdot 0.083} \cdot 0.079 \cdot 0.163 \cdot 0.803 = 0.619$$

The frequency is:

$$v = 1.038Hz \sqrt{\frac{0.619}{0.604 + 0.619}} = 0.739Hz > 0,08$$

And peak coefficient is:

$$k_p = \sqrt{2 \cdot \ln(v \cdot T)} + \frac{0.6}{\sqrt{2 \cdot \ln(v \cdot T)}} = \sqrt{2 \cdot \ln(0.739Hz \cdot 600s)} + \frac{0.6}{\sqrt{2 \cdot \ln(0.739Hz \cdot 600s)}} = 3.663 > 3.0$$

the turbulence intensity (from previous calculations) for h=36m, is:

$$I_v = \frac{k_I}{c_o(z) \cdot \ln\left(\dfrac{z}{z_o}\right)} = 0.209$$

However the structural coefficient $c_s c_d$ is:

$$c_s c_d = \frac{1 + 2 \cdot k_p \cdot I_v(z_e) \cdot \sqrt{B^2 + R^2}}{1 + 7 \cdot I_v(z_e)} = \frac{1 + 2 \cdot 3.668 \cdot 0.209 \cdot \sqrt{0.604 + 0.674}}{1 + 7 \cdot 0.209} = 1.094$$

- ***Procedure 2 for determining the structural* coefficient $c_s c_d$**

The background coefficient calculated using the formula:

$$B^2 = \frac{1}{1 + \dfrac{3}{2}\sqrt{\left(\dfrac{b}{L(z_e)}\right)^2 + \left(\dfrac{h}{L(z_e)}\right)^2 + \left(\dfrac{b}{L(z_e)} \cdot \dfrac{h}{L(z_e)}\right)^2}}$$

for

b=3.735m, h=60m and $L(z_e)$=105.435m (as defined previously).

$$B^2 = 0.539$$

The resonance response coefficient R^2 should be determined using formula:

$$R^2 = \frac{\pi^2}{2 \cdot \delta} \cdot S_L(z_e, n_{1,x}) \cdot K_s(n_{1,x})$$

where:

δ, S_L and F_L as identified in the procedure 1.

K_s is the size reduction function and calculated using the formula:

$$K_s(n) = \frac{1}{1 + \sqrt{(G_y \cdot \varphi_y)^2 + (G_z \cdot \varphi_z)^2 + \left(\dfrac{2}{\pi} \cdot G_y \cdot \varphi_y \cdot G_z \cdot \varphi_z\right)^2}}$$

$$\varphi_y = \frac{c_y \cdot b \cdot n}{v_m(z_e)} \qquad \varphi_z = \frac{c_z \cdot h \cdot n}{v_m(z_e)}$$

Note that, the constants G_y and G_z depend on the mode shape variation along the horizontal y-axis and vertical z-axes, respectively. The decay constants c_y and c_z are both equal to 11.5.

In Note 2 of ***Table C.1*** (EN1991-1-4) indicated that for chimneys with a uniform horizontal mode shape variation and a linear vertical mode shape variation is:

$$G_y = 1/2 \text{ and } G_z = 5/18$$

then,

$$\varphi_y = 0.778, \ \varphi_z = 12.492 \text{ and}$$

$$K_s(n) = 0.22$$

so:

$$R^2 = 0.837$$

The peak factor is calculated as in procedure 1, and is equal to

$$k_p = 3.688$$

Then, the structural factor is:

$$c_s c_d = \frac{1 + 2 \cdot k_p \cdot I_v(z_e) \cdot \sqrt{B^2 + R^2}}{1 + 7 \cdot I_v(z_e)} = \frac{1 + 2 \cdot 3.688 \cdot 0.209 \cdot \sqrt{0.539 + 0.837}}{1 + 7 \cdot 0.209} = 1.140$$

So since the dynamic coefficient calculated using both methods is less than 1.2 the approximate method of the total wind force calculation can be used. For the example purposes the higher the magnitude of the dynamic coefficient is used conservatively i.e. :

$$c_s c_d = 1.14$$

Table 2.7: Results of calculation structural factor $c_s c_d$ with procedures 1 and 2 which are proposed in EN 1991-1-4, Annex C.

Procedures (EN 1991-1-4, Annex B and C)	Structural factor $c_s c_d$
1	1.094
2	1.140

As can be seen, the second method of calculating the capacity coefficient gives more conservative results. Of course the variation among the results is limited in 4%, so both procedures can be considered reliable.

Consequently the first equation which gives the wind power is:

$$F_w = 1.14 \cdot c_f \cdot q_p(z_e) \cdot A_{ref}$$

The wind power, as was said initially, is calculated per distance 5m. The results are shown in ***Table 2.8.***

Table 2.8: Calculate the wind load on chimney.

Height (m)	c_{rz}	c_{0z}	kI	c_0	$[v_m]$	$[I_{vz}]$	$[q_{p(z)}]$ kN/m²	$[v_{ze}]$ m/s	Re	ψ_λ	c_{f0}	c_f	c_sc_d	q_{ref} (kN/m²)	c_e	Fw (kN/m²)	Fw (kN/m)
5,00	0,61	1,00	1,00	1,00	33,69	0,36	2,47	62,93	1,57E+07	0,72	0,73	0,52	1,14	1,93	1,28	1,48	5,53
10,00	0,76	1,00	1,00	1,00	41,99	0,29	3,30	72,69	1,81E+07	0,72	0,74	0,53	1,14	1,93	1,71	2,00	7,45
15,00	0,84	1,00	1,00	1,00	46,85	0,26	3,83	78,24	1,95E+07	0,72	0,74	0,53	1,14	1,93	1,98	2,32	8,68
20,00	0,90	1,00	1,00	1,00	50,29	0,24	4,22	82,13	2,05E+07	0,72	0,74	0,53	1,14	1,93	2,18	2,57	9,60
25,00	0,95	1,00	1,00	1,00	52,97	0,23	4,53	85,12	2,12E+07	0,72	0,74	0,54	1,14	1,93	2,34	2,77	10,34
30,00	0,99	1,00	1,00	1,00	55,15	0,22	4,79	87,55	2,18E+07	0,72	0,75	0,54	1,14	1,93	2,48	2,93	10,95
35,00	1,03	1,00	1,00	1,00	57,00	0,21	5,02	89,59	2,23E+07	0,72	0,75	0,54	1,14	1,93	2,60	3,08	11,49
40,00	1,05	1,00	1,00	1,00	58,60	0,20	5,22	91,35	2,27E+07	0,72	0,75	0,54	1,14	1,93	2,70	3,20	11,96
45,00	1,08	1,00	1,00	1,00	60,01	0,20	5,39	92,90	2,31E+07	0,72	0,75	0,54	1,14	1,93	2,79	3,32	12,39
50,00	1,10	1,00	1,00	1,00	61,27	0,20	5,56	94,29	2,35E+07	0,72	0,75	0,54	1,14	1,93	2,88	3,42	12,77
55,00	1,12	1,00	1,00	1,00	62,41	0,19	5,70	95,53	2,38E+07	0,72	0,75	0,54	1,14	1,93	2,95	3,51	13,12
60,00	1,14	1,00	1,00	1,00	63,45	0,19	5,84	96,67	2,41E+07	0,72	0,75	0,54	1,14	1,93	3,02	3,60	13,45

2.2.3. Vortex shedding and aeroelastic instabilities

According to the provisions of EN1993-3-2, the effect of the turbulence excitation to the chimney has to be determined and if aero elastic estability problems might occurs. EN1991-1-4 proposes two criteria (Anexx E). These criteria are as follows:

1. The effect of vortex shedding should be investigated when the ratio of the largest to the smallest crosswind dimension of the structure, both taken in the plane perpendicular to the wind, exceeds 6

2. The effect of vortex shedding need not be investigated when:

$$v_{crit,i} > 1,25 \cdot v_m$$

where:

$v_{crit,i}$ is the critical wind velocity for mode i, as defined in following paragraph

v_m is the characteristic 10 minutes mean wind velocity, at the cross section where vortex shedding occurs.

If it is assumed that y/b<0.1 then:

$$Lj = b \cdot 6 = 22.41m$$

therefore:

$$z_{v_m} = 60m - 21.4m / 2 \cong 48m$$

so,

$$v_m(48) = 60.778m / s$$

For this chimney:

$$\frac{h}{b} = \frac{60m}{3.735} = 16.06 > 6$$

Therefore from the note 1 the chimney need to investigated for the effect of vortex shedding

The critical wind velocity for bending vibration mode *i* is defined as the wind velocity at which the frequency of vortex shedding equals a natural frequency of the structure or a structural element and is given in formula:

$$v_{crit,i} = \frac{b \cdot n_{i,y}}{St}$$

where:

b   is the reference width of the cross-section at which resonant vortex shedding occurs and where the modal deflection is maximum for the structure or structural part considered

$n_{i,y}$ is the natural frequency of the considered flexural mode i of cross-wind vibration.

St   Strouhal number Strouhal.

the natural frequency of the considered flexural mode is:

$$n_1 = \frac{1000 \cdot 3.735}{60^2} \cdot \sqrt{1} = 1.038 [Hz]$$

From **Table E.1** (EN1991-1-4) the Strouhal number for circular section is:

$$St = 0.18$$

So because:

$$v_{crit,i} = \frac{b \cdot n_{i,y}}{St} = \frac{3.735m \cdot 1.038Hz}{0.18} = 21.539 m/s$$

$$\frac{v_{crit,i}}{v_m} = \frac{21.539 m/s}{60.778 m/s} = 0.354 < 1.25$$

the chimney need to investigated for the effect of vortex shedding

The critical wind velocity for ovalling vibration mode i is defined as the wind velocity at which the frequency of vortex shedding equals a natural frequency of the structure or a structural element and is given in formula:

$$v_{crit,i} = \frac{b \cdot n_{i,0}}{2 \cdot St} \quad (4.\ 2)$$

$n_{i,o}$ The fundamental ovalling frequency.

The fundamental ovalling frequency $n_{1,0}$ of a long cylindrical shell without stiffening rings may be calculated using formula:

$$n_{1,0} = 0.492 \cdot \sqrt{\frac{t^3 \cdot E}{\mu_s \cdot (1-v^2) \cdot b^4}}$$

where:

E   is Young's modulus in $[N/m^2]$

t   is the shell thickness in [m]

v   is Poisson ratio

μ_s is the mass of the shell per unit area in $[kg/m^3]$

b   is the diameter of the shell in [m]

as elasticity module E is considered the one reduced, cause of the temperature effect, while is assumed as an average shell thickness, equal to t=9.1mm (reduced due to corrossion).

$$\mu_s = \frac{668.724 kN \cdot 100}{60m \cdot \pi \cdot 3.735} = 94.99 \frac{kg}{m^2}$$

and:

$$n_{1,0} = 0.492 \cdot \sqrt{\frac{t^3 \cdot E}{\mu_s \cdot (1-v^2) \cdot b^4}} = 0.492 \cdot \sqrt{\frac{(9.1mm)^3 \cdot 1.4x10^{11} N/m^2}{94.99 kg/m^2 \cdot (1-0.3^2) \cdot (3.735m)^4}} = 1.432 Hz$$

so:

$$v_{crit,i} = \frac{b \cdot n_{i,0}}{2 \cdot St} = \frac{3.735m \cdot 1.432 Hz}{2 \cdot 0.18} = 14.899 m/s$$

therefore,

$$\frac{v_{crit,i}}{v_m} = \frac{14.899 m/s}{60.778 m/s} = 0.245 < 1.25$$

Therefore, needs further testing for elliptical vibration by turbulent agitation. As was shown by the above, the criteria in this case are not met. Consequently is required to check the chimney over aeroelastics turbulent agitation and instability.

The effect of vibrations induced by vortex shedding should be calculated from the effect of the inertia force per unit length $F_w(s)$, acting perpendicular to the wind direction at location *s* on the structure and given in formula:

$$F_w(s) = m(s) \cdot (2 \cdot \pi \cdot n_{i,y})^2 \cdot \Phi_{i,y}(s) \cdot y_{F,max}$$

where:

m(s)   is the vibrating mass of the structure per unit length [kg/m]

$n_{i,y}$ is the natural frequency of the structure

$\Phi_{i,s}(s)$ is the mode shape of the structure normalized to 1 at the point with the maximum displacement

$Y_{F,max}$ is the maximum displacement over time of the point with $\Phi_{i,s}(s)$ equal to 1.

In order to determine the range of transverses vibration, two methods are proposed by EN1991-1-4 (Annex E). National annexes does not indicate which of the two methods should be used. The same annex (par. E.1.5.3) provides details of the use of methods. EN1991-1-4 notes that these two methods cannot take any comparison. In this study the calculation of the range of transverse vibration is with both methods in order to indicate any possible deviation.

- **Approach 1 for the calculation of the cross wind amplitudes**

Is supposed that: $\dfrac{y_F}{b} < 0.1$, where $\mathbf{y_F}$ is the vibration range. The active correlation length comes from

the *Table E.4. (EN 1991-1-4)*:

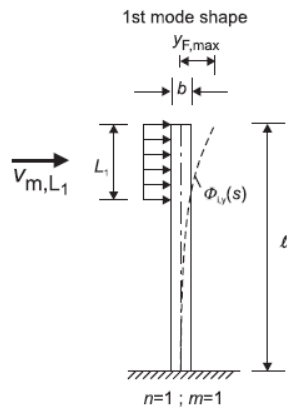$$\frac{L_j}{b} = 6 \Rightarrow L_j = 6 \cdot b = 6 \cdot 3.735 = 22.40m$$

1st mode shape

Figure 2.2: Examples for application of the correlation length Lj.

The value of average wind velocity on height z=60 – 22.41/2=48.8m is:

$$v_{mL,j} = 60.98 m/s$$

The critical wind velocity ratio is:

$$\frac{v_{crit,j}}{v_{m,L,j}} = \frac{21.593}{60.98} = 0.354 < 0.83$$

The lateral force coefficient, according the Table E.3, is:

$$c_{lat} = c_{lat,o}$$

where $c_{lat,o}$ basic value of c_{lat}, apparent from Figure E.2 for circular cylinders, versus the Reynolds number, Re, which is calculated using the formula:

$$\mathrm{Re}(v_{crit,j}) = \frac{b \cdot v_{(z_e)}crit, j}{v} = \frac{3.735m \cdot 60.98m/5}{15 \cdot 10^6} = 5.377 \cdot 10^6$$

Therefore, for Re=5.377x10^6 is $c_{lat,o}$=0.2. ie:

$$c_{lat} = c_{lat,o} = 0.2$$

The largest displacement $y_{F\ max}$, can be calculated using formula:

$$\frac{y_{F,\max}}{b} = \frac{1}{St^2} \cdot \frac{1}{S_c} \cdot K \cdot K_W \cdot c_{lat}$$

where:

St   is the Strouhal number

Sc   is the Scruton number

Kw   is the effective correlation length factor

K   is the mode shape factor

For this chimney:

$$St = 0.18 \quad (\textbf{\textit{Table E.1}})$$

$$Sc = \frac{2 \cdot \delta_s \cdot m_{i,e}}{\rho \cdot b^2}$$

where,

$m_{i,e}$: η is the equivalent mass m_e per unit length for mode i:

$$m_e = \frac{\int_0^l m(s) \cdot \Phi_1^2(s)\,ds}{\int_0^l \Phi_1^2(s)\,ds}$$

where,

$\Phi_1(z)$: is the first mode

They approach that the mass is distributed according the height :

$$m_{i,e} = \frac{W_t}{g \cdot L} = \frac{668.742 kN}{9.81\frac{m}{s^2} \cdot 60m} = 1.137 \frac{kN \cdot s^2}{m^2}$$

Therefore the Struton number is:

$$Sc = \frac{2 \cdot \delta_s \cdot m_{i,e}}{\rho \cdot b^2} = 2.607$$

The factors K και K_w are given in Table E.5:

$$K = 0.13$$

$$K_W = 3 \cdot \frac{Lj/b}{\lambda}\left[1 - \frac{Lj/b}{\lambda} + \frac{1}{3}\cdot\left(\frac{Lj/b}{\lambda}\right)^2 \right] \quad \text{όπου } \lambda = L/b$$

$$K_W = 3 \cdot \frac{Lj/b}{\lambda}\left[1 - \frac{Lj/b}{\lambda} + \frac{1}{3}\cdot\left(\frac{Lj/b}{\lambda}\right)^2 \right] = 0.754$$

So:

$$\frac{y_{F,\max}}{b} = \frac{1}{St^2} \cdot \frac{1}{S_c} \cdot K \cdot K_W \cdot c_{lat} = \frac{1}{0.18^2} \cdot \frac{1}{1.831} \cdot 0.13 \cdot 0.754 \cdot 0.2 = 0.33$$

So the initial assumption that $\frac{y_F}{b} < 0.1$ does not valid. The process is repeated with $\frac{y_F}{b} = 0.33$. The repetitions continue until there is a convergence. The results of the repetitions are shown in **Table 2.9.**

As can be seen from **Table 2.9** there is a convergence at value:

$$\frac{y_F}{b} = 0.269$$

Consequently, the maximum value of the transverse vibration can be calculated using the formula:

$$y_{Fj} = 0.269 \cdot b = 0.269 \cdot 3.735m = 1.006m$$

- **Approach 2, for the calculation of the cross wind amplitudes**

The characteristic maximum displacement at the point with the largest movement is calculated using the formula:

$$y_{\max} = \sigma_y \cdot k_p$$

where:

k_p is the peak factor

σ_y is the standard deviation of the displacement and may be calculated using the formula:

$$\frac{\sigma_y}{b} = \frac{1}{St^2} \cdot \frac{C_c}{\sqrt{\frac{Sc}{4 \cdot \pi} - Ka \cdot \left(1 - \left(\frac{\sigma_y}{b \cdot a_L}\right)^2\right)}} \cdot \sqrt{\frac{\rho \cdot b^2}{m_e}} \cdot \sqrt{\frac{b}{h}}$$

όπου:

C_c is the aerodynamic constant dependent on the cross-sectional shape, and for a circular cylinder also dependent on the Reynolds number Re as given in TableE.6 (for *Re ≥ 10⁶*, C_c=0.01.)

Ka   is the aerodynamic damping parameter as given in Table E.6 *(For Re ≥ 10⁶ Ka=1).*

a_L is the normalised limiting amplitude giving the deflection of structures with very low damping. For Re ≥ 10⁶ a_L=0.4.

St   is the Strouhal numbe, St=0.18 (Πίνακας Ε.1)

ρ   is the air density under vortex shedding conditions. ρ=1.25kg/m³.

m_e is the effective mass per unit length

$$m_e = \frac{W_t}{L} = \frac{502.924kN}{60m} = 8.382 \frac{kN}{m}$$

h,b   is the height and width of structure.

Table 2. 9: Result of repetition calculated the characteristic maximum displacement using the approach 1.

Repetition	y_F/b	Lj (m)	z (m)	v_{mLj} (m/s)	v_{criti} (m/s)	v_{mLj}/v_{criti}	Re	c_{lat}	me (kN·s²/m²)	Sc	St	K	Kw	y_F/b
-	<0,1	22,400	48,800	60,980	21,59	0,354	5,38E+06	0,20	1,137	2,61	0,18	0,13	0,754	0,232
1	0,232	28,329	45,836	60,226	21,59	0,359	5,38E+06	0,20	1,137	2,61	0,18	0,13	0,853	0,263
2	0,263	29,695	45,152	60,046	21,59	0,360	5,38E+06	0,20	1,137	2,61	0,18	0,13	0,871	0,268
3	0,268	29,946	45,027	60,013	21,59	0,360	5,38E+06	0,20	1,137	2,61	0,18	0,13	0,874	0,269
4	0,269	29,990	45,005	60,006	21,59	0,360	5,38E+06	0,20	1,137	2,61	0,18	0,13	0,875	0,269

The solution to formula is:

$$\left(\frac{\sigma_y}{b}\right)^2 = c_1 + \sqrt{c_1^2 + c_2}$$

Where the constants c_1 and c_2 are given by:

$$c_1 = \frac{a_L^2}{2} \cdot \left(1 - \frac{S_c}{4 \cdot \pi \cdot K_a}\right) = 0.063 \qquad c_2 = \frac{\rho \cdot b^2}{m_e} \cdot \frac{a_L^2}{K_a} \cdot \frac{C_c^2}{St^4} \cdot \frac{b}{h} = 1.456x10^{-5}$$

Based on the above is:

$$\left(\frac{\sigma_y}{b}\right)^2 = c_1 + \sqrt{c_1^2 + c_2} = 0.252$$

therefore:

$$\sigma_y = 1.874m$$

The peak factor calculated using the formula:

$$k_p = \sqrt{2} \cdot \left(1 + \frac{1.2}{\tan\left(0.75 \cdot \frac{Sc}{(4 \cdot \pi \cdot K_a)}\right)}\right)$$

However the proposed formula presents problems which confirmed by Zdravkovich M.M. and Kawecki J. (2007)[9]. For this reason the peak rate is calculated from the formula 7.4.14 proposed byDyrbye and Hansen (1996)[2]:

$$k_p = \sqrt{2} \cdot \left(1 + 1.2 \cdot \tan^{-1}\left(0.75 \cdot \left(\frac{Sc}{S_a}\right)^4\right)\right)$$

where:

$$Sa = \frac{2 \cdot \delta_\alpha \cdot m_e}{\rho \cdot b^2} = 8.578$$

(δ_α=0.086,by previous calculations)
so:

$$k_p = 1.418$$

and

$$y_{max} = 1.874m \cdot 1.418 = 2.671m$$

Peak factor kp versus the aerodynamic αεροδυναμικής damping are illustrated in ***Figure 2.3***. Furthermore, it is worth noting that CICIND[1] propose the following value for peak factor k_p:

$$k_p = 1.5 \, \acute{o}\tau\alpha\nu \quad \sqrt{c_1 + \sqrt{c_1^2 + c_2}} > 0.04$$

$$k_p = 4 \text{ όταν } \sqrt{c_1 + \sqrt{c_1^2 + c_2}} < 0.04$$

For this chimney $\sqrt{c_1 + \sqrt{c_1^2 + c_2}} = 0.51 > 0.04 \text{ άρα}$

$$k_p = 1.5$$

and

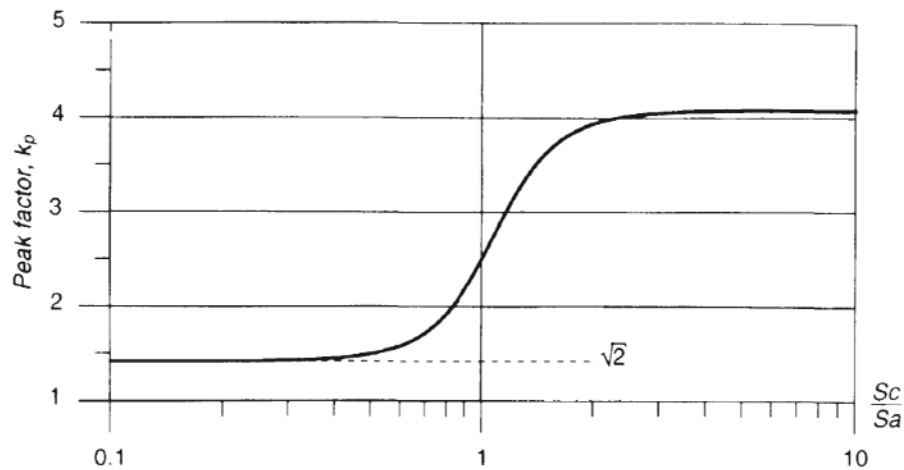$$y_{max} = 1.874m \cdot 1.5 = 2.811m$$

Figure 2.3: Peak factor kp versus the aerodynamic damping

Below is a table summarizing the calculated results from the range of vibration at the top of the chimney, using the three methods.

Table 2. 10: Maximum vibration range at the top of the chimney using 1 and 2 methods which EN 1991-1-4 and CICIND- Mode Code propose

	EN 1991-1-4, Μέθοδος 1	EN 1991-1-4, Μέθοδος 2	CICIND
y_{Fmax}	1.006m	2.671m	2.811m

As can be seen from the results and according to Zdravkovich M.M. and Kawecki J. (2007)[9] method 1 which EN1991-1-4 proposes underestimate a lot the maximum vibration range (in this case, the difference between the two methods is around 62%). From these two, is proposed the calculation of the vibration range according to method 2. Consequently,

$$y_{\max} = 2.671m$$

The fundamental modal Φ1(z) chimney, based on the ground is calculated by the formula:

$$\Phi_1(z) = \left(\frac{z}{h}\right)^{\zeta}$$

For steel chimneys is ζ=2according to Paragraph F.3.(EN1991-1-4)

As mentioned, the effect of turbulent agitation is expressed through the inertia power per length unit, $F_{i,j}$, which is vertical to the wind direction at j point of manufacture, according to the formula:

$$F_w(s) = m(s) \cdot (2 \cdot \pi \cdot n_{i,y})^2 \cdot \Phi_{i,y}(s) \cdot y_{F,\max}$$

Where m(s) the vibrating mass.

For the calculation of these forces is assumed that the mass is evenly distributed vertically. So:

$$m(s) = \frac{W_t}{g \cdot h} = \frac{668.724kN}{9.81\frac{m}{s^2} \cdot 60m} = 1.137 \frac{kN \cdot s^2}{m^2}$$

Table 2.11: Vortex shedding action F_w

z(m)	Φ₁(z)	me (kN·s²/m²)	*max y_F*	$n_{i,y}$ (Hz)	$F_{i,j}$ (kN/m)	L_{arc} (m)	$F_{i,j}$ (kN/m2)
2,5	0,002	1,137	2,671	1,038	0,22	2,440	0,09
10,0	0,028	1,137	2,671	1,038	3,59	2,440	1,47
24,0	0,160	1,137	2,671	1,038	20,67	2,440	8,47
36,0	0,360	1,137	2,671	1,038	46,50	2,440	19,06
47,0	0,614	1,137	2,671	1,038	79,27	2,440	32,49
58,0	0,934	1,137	2,671	1,038	120,71	2,440	49,47
60,0	1,000	1,137	2,671	1,038	129,18	2,440	52,94

Table 9.14. shows calculations of the inertial force F_w, per length unit of construction, at the positions where is a change in the shell thickness of the chimney (this assists the process of enforcements charge in the ADINA software as will be presented in the next section). At the same time, the force is assigned on the surface of the shell as equally distributed pressure which acts in the region where negative pressure is appeared tranverse in the wind flow. The length is calculated as:

$$\mu^o = 105^o - 30^o = 75^o$$

(30° : position of a zero pressure, 105° : position of flow separation for Re=x10⁷)

So the arc length is:

$$L_{arc} = \frac{\pi \cdot \dfrac{d}{2}}{180^o} \mu^o = \frac{\pi \cdot \dfrac{3.735m}{2}}{180^o} 75^o = 2.44m$$

2.3. Earthquake forces

In this section are calculated the earthquake actions. Then, is calculated the range of design which will calculate the earthquake actions for a linear elastic analysis.

The horizontal design elements are determined by the design spectrum, whose ordinates for each fundamental period T [sec] are calculated by the formulas:

$$0 \leq T \leq T_B : S_d(T) = a_g \cdot S \cdot \left[\frac{2}{3} + \frac{T}{T_B} \left(\frac{2,5}{q} - \frac{2}{3} \right) \right] \text{(5. 1)}$$

$$T_B \leq T \leq T_C : S_d(T) = a_g \cdot S \cdot \frac{2,5}{q} \text{(5. 2)}$$

$$T_C \leq T \leq T_D : S_d(T) \begin{cases} = a_g \cdot S \cdot \dfrac{2,5}{q} \left[\dfrac{T_C}{T} \right] \\ \geq \beta \cdot a_g \end{cases} \text{(5. 3)}$$

$$T_D \leq T : S_d(T) \begin{cases} = a_g \cdot S \cdot \dfrac{2,5}{q} \left[\dfrac{T_C T_D}{T} \right] \\ \geq \beta \cdot a_g \end{cases} \text{(5. 4)}$$

where:

$S_d(T)$ is the design spectrum

T   is the vibration period of a linear single-degree-of-freedom system

a_g is the design ground acceleration on type A ground A($a_g = \gamma_I \, a_{gR}$)

T_B is the lower limit of the period of the constant spectral acceleration branch

T_C is the upper limit of the period of the constant spectral acceleration branch

T_D is the value defining the beginning of the constant displacement response range
         of the spectrum

S   is the soil factor

η   is the damping correction factor with a reference value of η=1 for 5% viscous
         damping

q   is the behaviour factor

β   is the lower bound factor for the horizontal design spectrum (β=0,2)

According to the new earthquake hazard map of Greece, Syros is located in seismic hazard zone α=0.16, so the maximum ground acceleration is A=0.16g.

The construction of the chimney is of paramount priority importance, therefore the importance coefficient gets the value γ_I=1.4.

The basic coefficient behavior q_o is equal to 1.5. There are not any eccentricities on the shell. Therefore the coefficient behavior is:

$$q = q_o \cdot k_r \geq 1.5$$

$$q = 1.5 \cdot 1.0 = 1.5$$

Moreover, is an A territorial category A, so are:

Territorial Type	S	$T_B(s)$	$T_C(s)$	$T_D(s)$
A	1,0	0,15	0,4	2,0

Figure **9.5** is shown the spectrum of design, type 1.
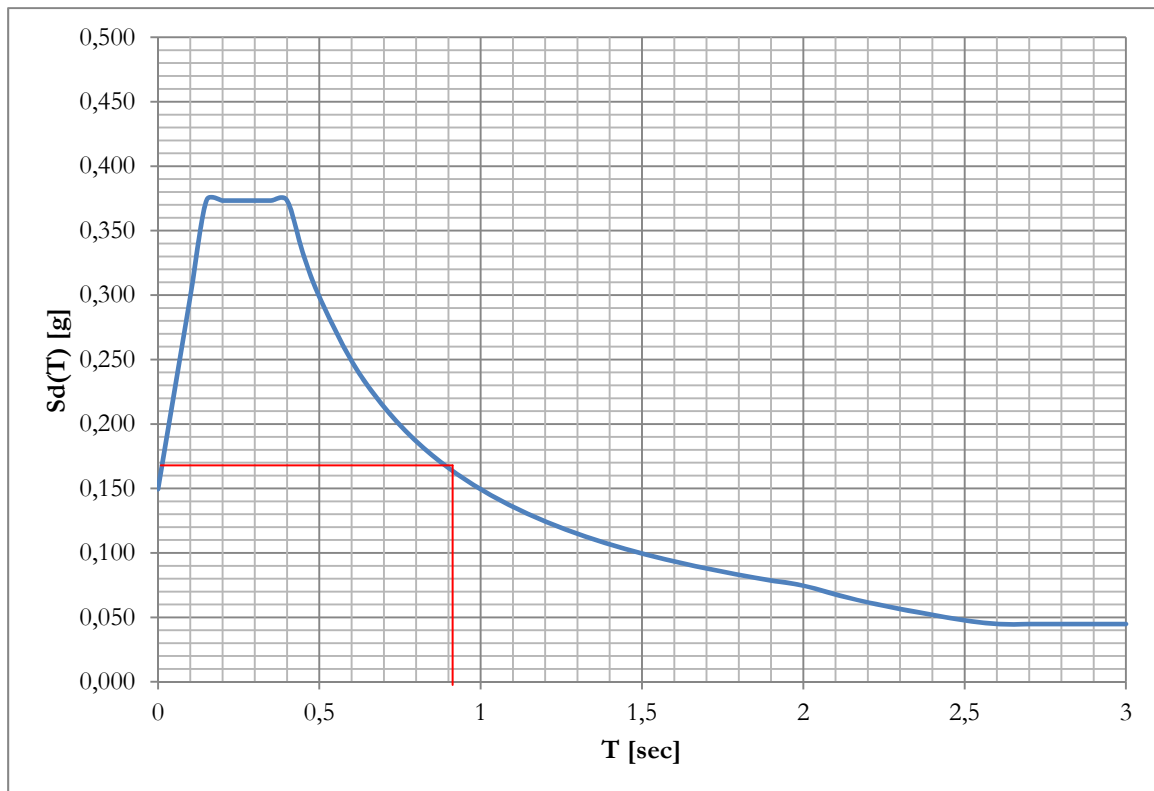
Figure 2.4: Design spectra for elastic analysis for soil type A, 5% dumping, seismic hazard zone 1 and importance coefficient γ_I=1.4, by EN1998-1.

For structural symmetry reasons only the next seismic combination will be used:

$$1.0G + 0.3Q + 1.0E_x + 0.3E_y$$

For simplifying reasons the analysis under seismic loads, will be held for the linear analysis with an equivalent static method. For this reason, are calculated the participation rates of the masses to retrospectively calculate the inertial force due to seismic excitation. ***Table 9.15*** shows the participation rates for the first 6 modals (with shell finate elements).

Table 2.12: Mass participation rates for the first six modals of the chimney

Modal	mass participation coefficient, X direction	mass participation coefficient, Y direction	mass participation coefficient, Z direction
1	4,71E+05	-2,18E+05	5,22E-02
2	2,18E+05	4,71E+05	2,10E-02
3	2,85E+05	-1,67E+05	3,36E-01
4	-1,67E+05	-2,85E+05	1,19E-01
5	1,97E-01	1,58E-01	1,76E-01
6	-1,51E-01	3,26E-01	3,44E-01

As can be seen, the first two modals are equal and are taking into account the higher mass coefficient for the X and Y directions. This is taken as "dominant Eigen frequency" as the first frequency which will be:

$$F = 1.087 Hz$$

$$T = \frac{1}{F} = 0.920 \sec$$

Consequently from the range design is calculated the structural acceleration:

$$Sd(T = 0.920) = 0.16g$$

So for every different section thickness of the structure, is calculated the inertia force which is supposed to act in construction, per length unit by the formula:

$$F_{Ed_i} = 2 \cdot G \cdot \pi \cdot r \cdot t_i \cdot Sd(T = 0.920)$$

where:

G   weight of the material in kg/m^3

r   radius

t_i shell thickness

the corresponding calculations are given in ***Table 9.16.***

It is mentioned that the inertia force will be assigned at X and Y directions with coefficient as have been defined by the seismic combination. In the static model of shell finite elements the inertia force becomes pressure to avoid the phenomena of stress concentration on shell elements.

Table 2.13: Inertia forces on the structure due to earthquake.

Element group	Length (m)	Thickness (mm)	Inertial force kN/m	Inertial force kN/m² (X direction n)*	Inertial force kN/m³ (Y direction)*
1	10	15	2,21	1,13	0,91
2	14	14	2,06	1,05	0,85
3	12	9	1,33	0,68	0,54
4	22	7	1,03	0,53	0,42
5	2	5	0,74	0,38	0,30

*The surface width by which the force was normalized, corresponds to the width when the wind loads where distributed (L_x=1.956m, L_y=2.44m).

In scenario of non-lineal analysis it is not possible to use neither the equivalent static nor the spectral method of calculating seismic loads. In this case close distance recorded accelerograph is used. It is noted that accelerograph should be deduced to the maximum seismic designed acceleration which is in this case 0,16g.

2.4. Thermal Action

The influence of the temperature changes occurs with the impairment of mechanical properties of structural steel. For this example is considered as a maximum shell temperature 50oC. The mechanical properties of steel S355 are shown on Table 9.17.

Table 2.14: Mechanical properties of steel CORTEN S355 at temperature 50° C

Mechanical properties	Symbol	Price	Measurment Units
Elasticity Module	E	170.00	GPA
Poisson Ratio	ν	0.33	-
Density	ρ	7850.00	Kg/m^3
Yield Capacity	fy	345.00	MPa
Ultimate Capacity	fu	-	MPa

Generally, a consistent perimetric change on the shell temperature, is not likely to make any further intensive sizes, since the construction can free expand and shrink. An uneven temperature distribution might be presented which will stress the body, but for simplification reasons, this parameter is overlooked

3

MODELING, ANALYSYS AND DESIGN OF THE CHIMNEY

The chimney was evaluated for the stability and serviceability criteria proposed by EN1993-1-6. The boundary conditions LS1 - plastic failure or tensile breakage, LS2 - Plasticity in cyclic loading, LS3- Buckling and LS4 - Fatigue were evaluated. All checks are performed using the analytical formulas but also through non-linear numerical analysis.

For the purposes of the non-linear analyses, the steel chimney was simulated with the finite element software ADINA. Two static simulants were developed; ie static simulant 1 (S.S.1) using shell finite elements and static simulants 2 (S.S.2): using bar finite elements.

In S.S.1, a preliminary analysis of the effect of dimensional lattice of finite element on the results was investigated. After several testings, a grid of nine-node finite elements with dimensions 0.70m x 0.70m was chosen. Joint conditions were used at the base with rotational release in the directions X and Y. Also designated static diaphragms were used in the positions of thickness change of the shell in order to simulate this way the rigid, in their level, frontal plates used for the connections of the different parts. The flanges have annular shape and thickness about 1-3cm. For this reason, they are considered to be rigid at their level.
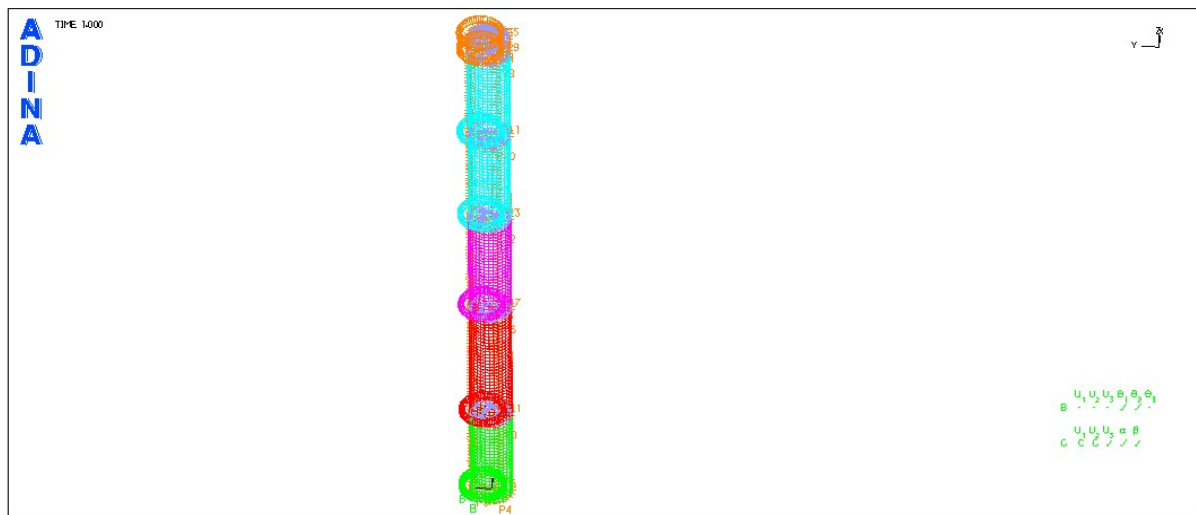
Figure 3. 1:Static stimulant with shell elements
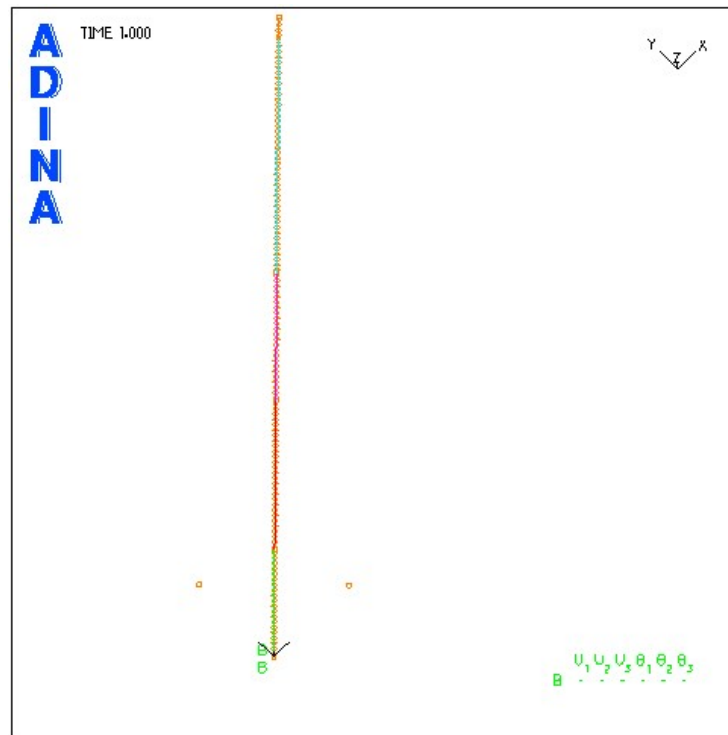
Figure 3. 2: Static stimulant with bar elements

The S.S.2 was divided into equal parts of 0.20m. Fully anchorage conditions were considered at the base. In ***Figures 2*** and ***3*** the static simulants are shown, as simulated in the software ADINA. Different colors designate different thicknesses of the elements. Initially, static analysis was performed in both static simulants in order to determine their characteristics and natural frequencies. In Figure 4-13 the first five modals. Respectively, in ***Table 3*** are the values of natural frequency. The natural frequency of the chimney was also calculated using the function F3 proposed

by EN1991-1-4. As derives from the figures, but also from the values, the first four modals that were calculated for the two static simulants are matching. Very good was also the estimation of the first modal calculated by the formula of EN1991-1-4.

Table 3. 1:Modals and natural frequencies in as calculated for S.S.1 & S.S.2 and the formula of EN1991-1-4.

Modal	S.S.1: shll finite elements, natural frequency [Hz]	S.S.2: bar finite elements, natural frequency in [Hz]	EN1991-1-4, natural frequency in [Hz]
1st modal - flexural	1.087	1.089	1.038
2nd modal - flexural	1.087	1.089	----
3rd modal - flexural	5.509	5.690	----
4th modal - flexural	5.509	5.690	----
5th modal - elleptical	9.516	12.560	----

The fifth modal of the S.S. finite element shell is elliptical and varies in value from the corresponding "fifth" modal of the S.S. using bar finite elements. Elliptic modal, understandably, cannot be observed using S.S.2 due to bar elements. At this point, it should also be noted that the simulation of frontal plates as diaphragms in the mounting position of the chimney's body plays a key role in the modal analysis of the structure. Without the diaphragms, the modals arising in S.S.1 are all elliptical.
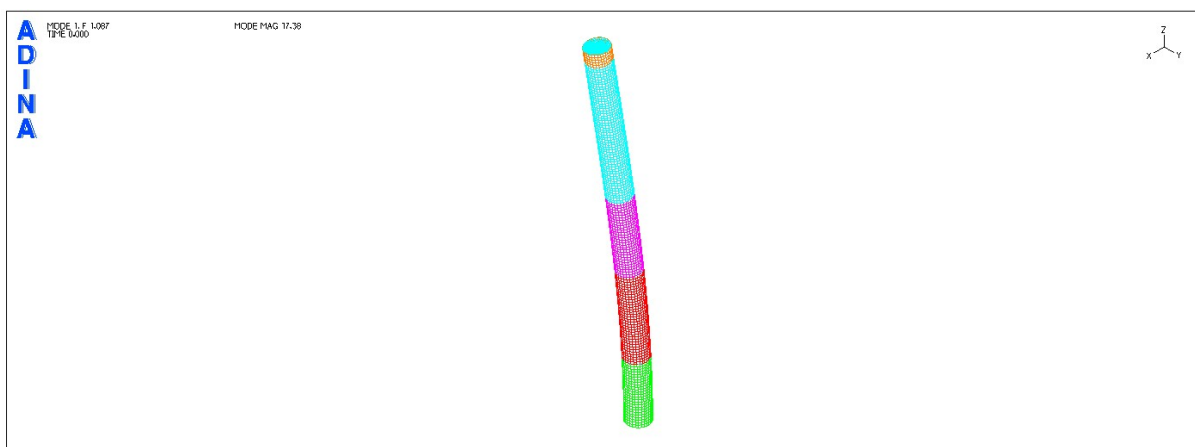
Figure 3. 3: Static stimulant with shell finite elements, 1st modal
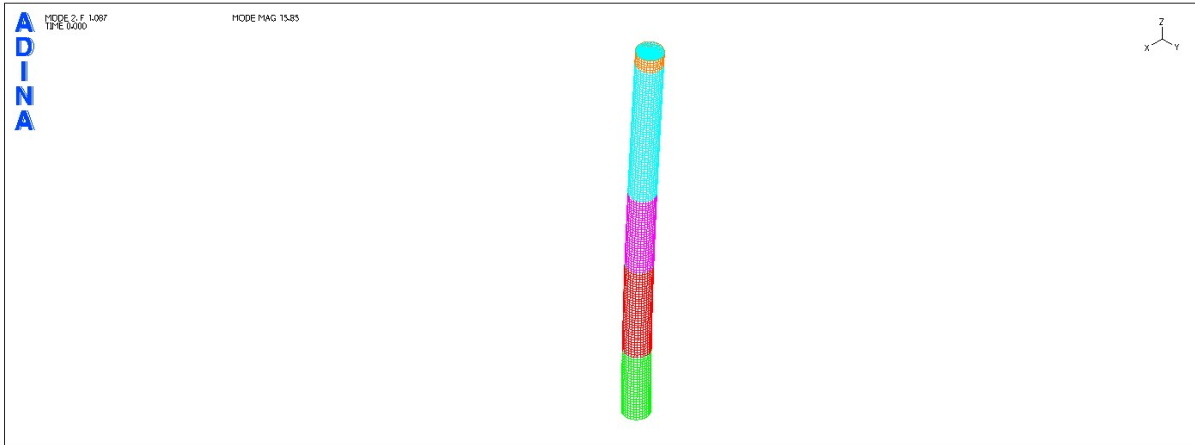
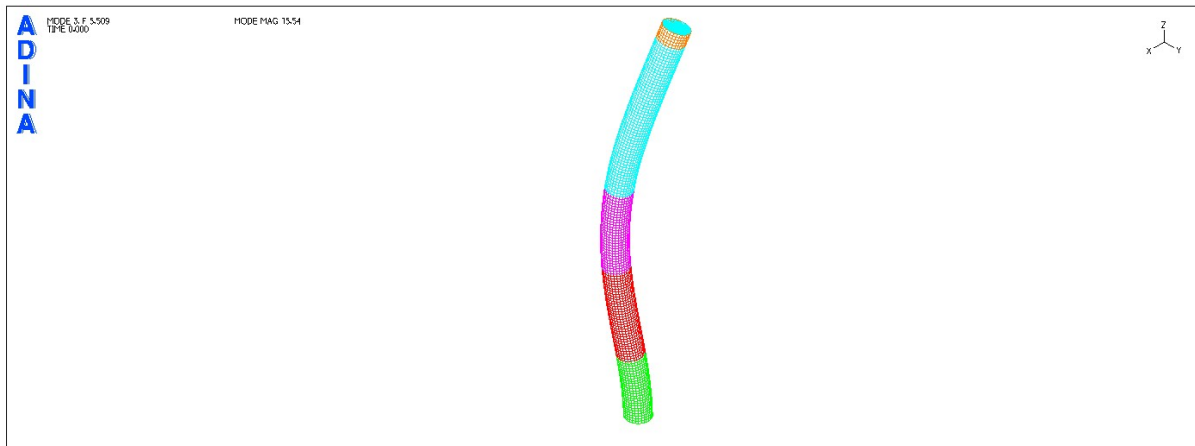***Figure 3. 4:*** Static stimulant with shell finite elements, 2nd modal

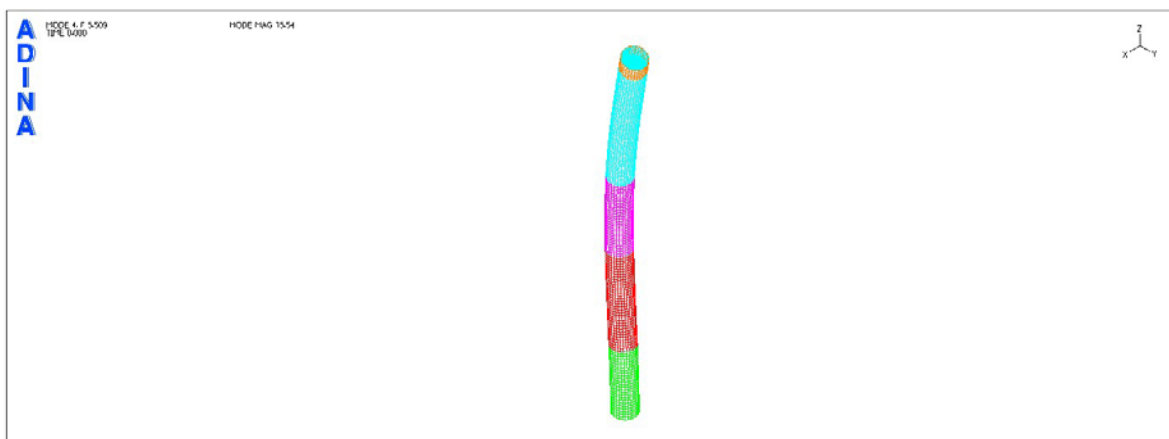***Figure 3. 5:*** Static stimulant with shell finite elements, 3rd modal

Figure 3. 6: Static stimulant with shell finite elements, 4th modal
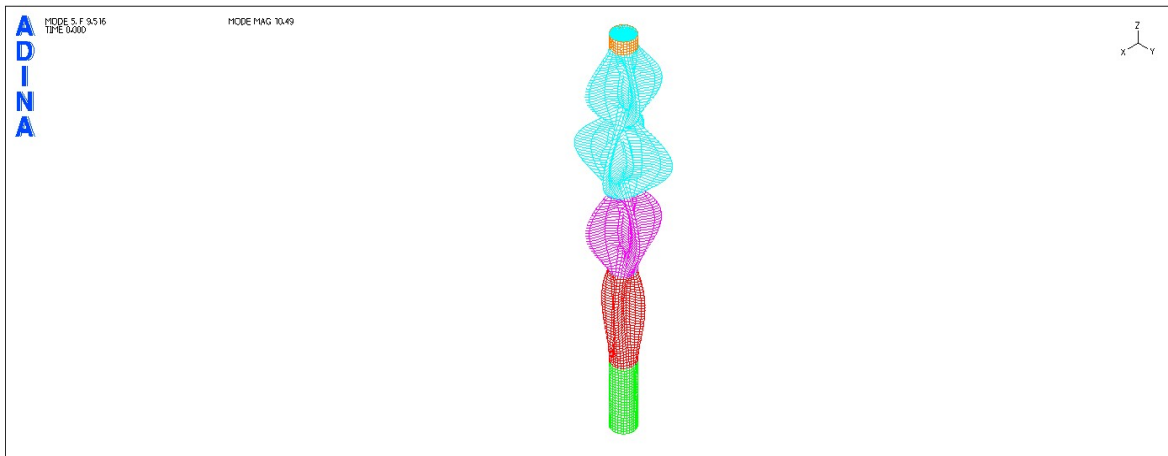
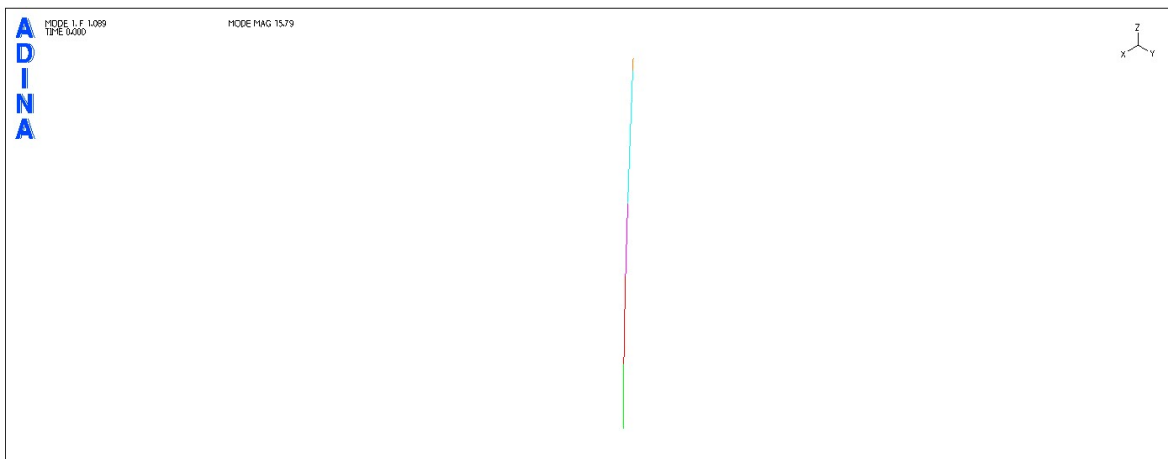***Figure 3. 7:*** Static stimulant with shell finite elements, 5th modal

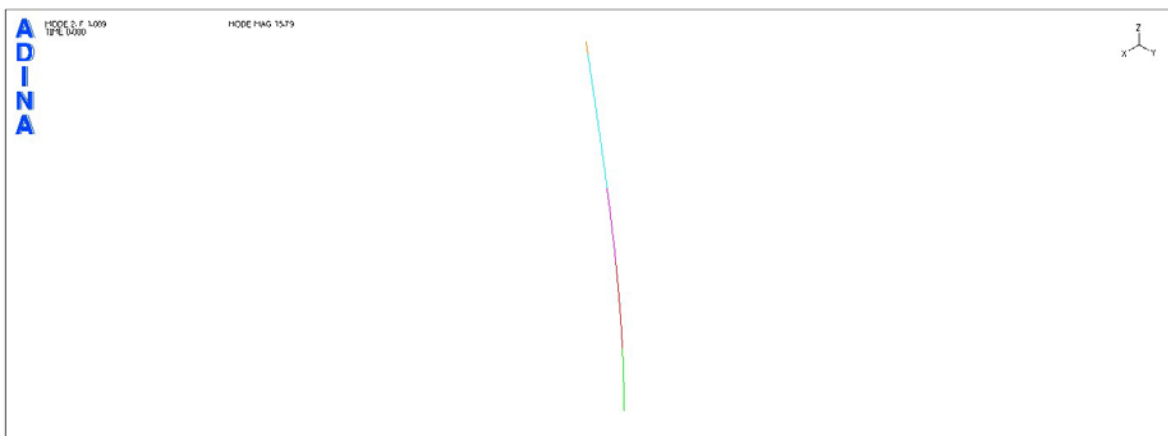***Figure 3. 8:*** Static stimulant with bar finite elements, 1st modal
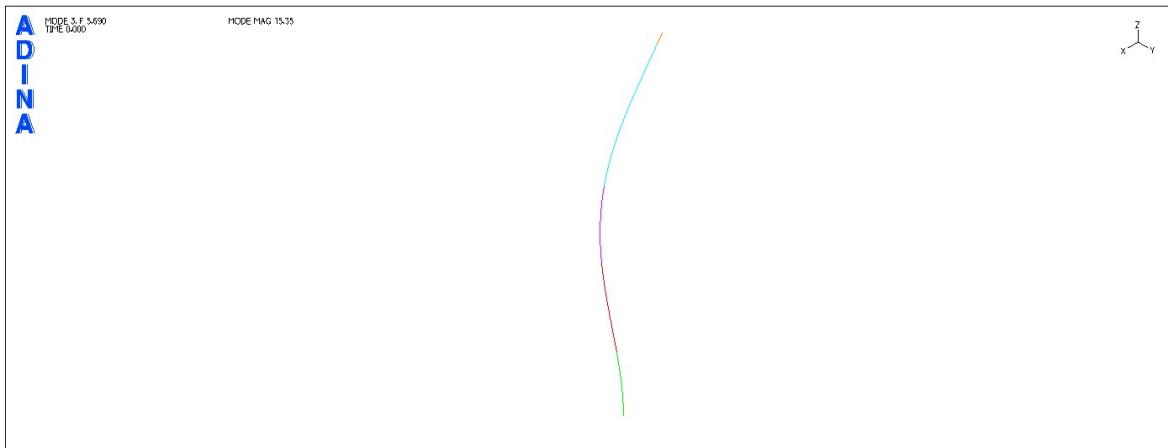

Figure 3. 9: Static stimulant with bar finite elements, 2nd modal

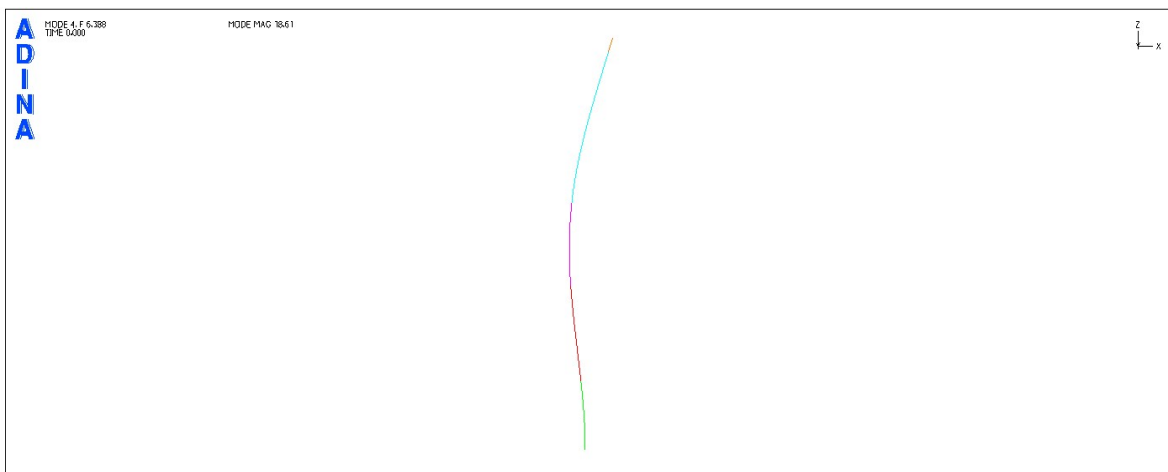**Figure 3. 10:** Static stimulant with bar finite elements, 3rd modal

Figure 3. 11: Static stimulant with bar finite elements, 4th modal
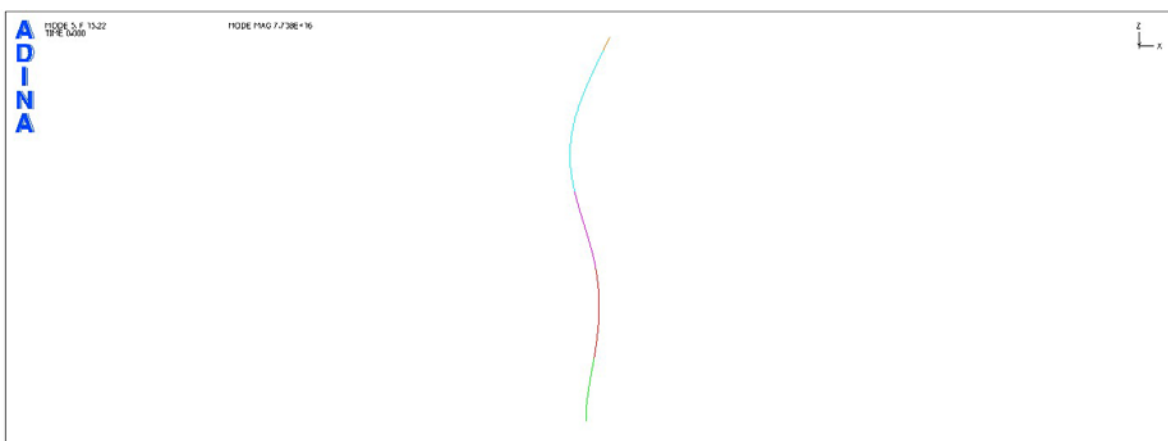

Figure 3. 12: Static stimulant with bar finite elements, 5th modal

The limit state analysis is performed for the four limit states proposed by EN1993-1-6 (Strength and stability of shells). For the corresponding limit state conditions, all the proposed check methods are used. Initially, however, for purposes of simplification of the calculations and analyses, a preliminary elastic analysis was carried out in order to determine worst case scenario. The chimney is evaluated for the combined loads with main load the wind and for the seismic combination.

In the following Figures, the analysis results from two load combinations are presented. It's obvious from the results that the worst combination is the one with the wind as the main load. As understood, the structure because of its relatively small mass is more prone to the wind load, than to any seismic excitation.

Therefore, all subsequent analyses performed, for purposes of simplification, were based on the load combinations with the wind as the main load. From the preceding preliminary analyses, it appears that the von Misses stress is at the yielding capacity F_{yd} of the steel S355. So it was considered appropriate to increase the thickness of the shells near the base. The new shell thicknesses are presented in *Table 4*.
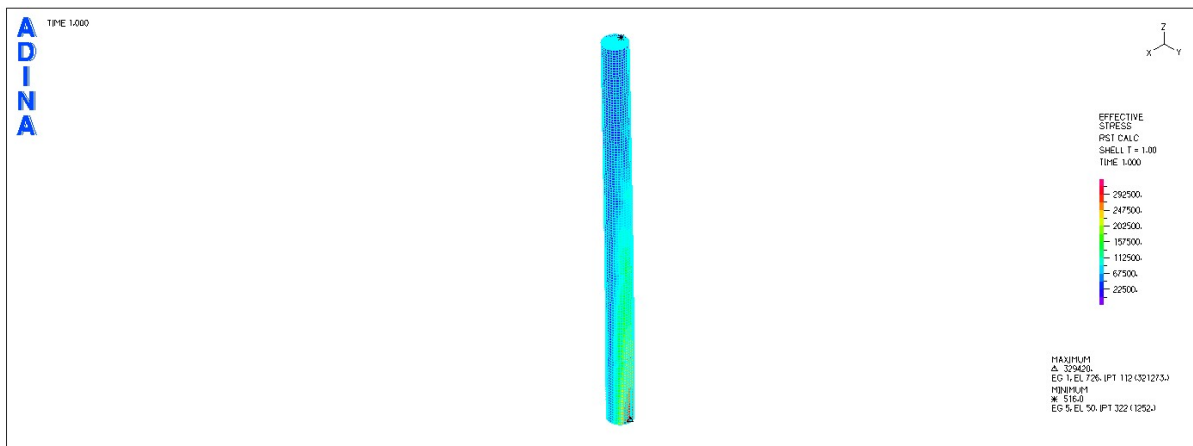

Figure 3. 13: Analysis results for the static stimulant with shell finite elements for load combination with main load the wind. von Misses stress = 329.420 MPa
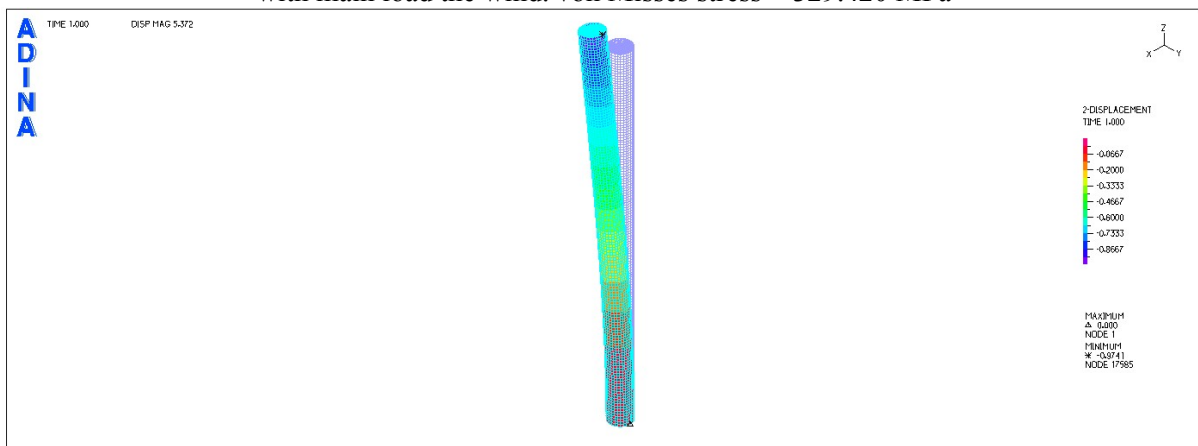

Figure 3. 14*:* Analysis results for the static stimulant with shell finite elements for load combination with main load the wind. Maximum displacement 0.97cm
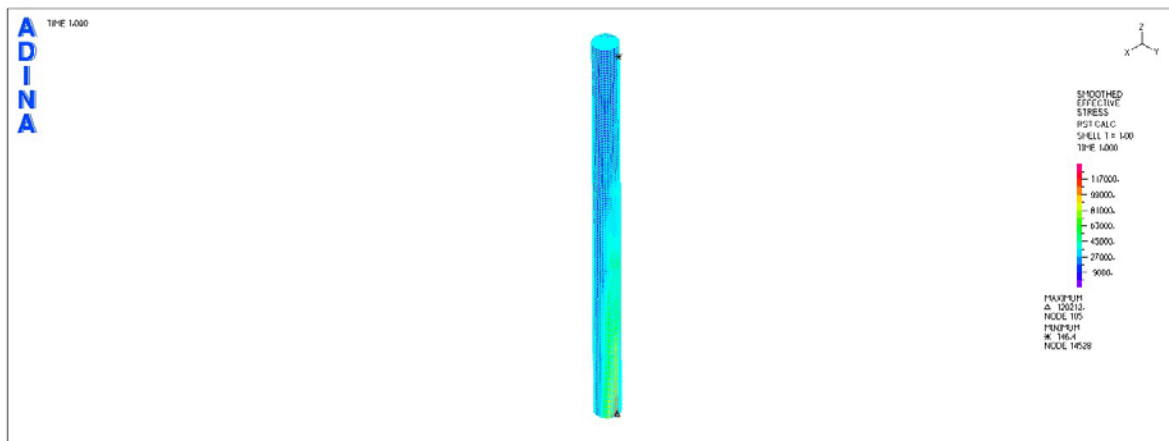
Figure 3. 15: Analysis results for the static stimulant with shell finite elements for the seismic load combination. von Misses stress = 120.212 MPa
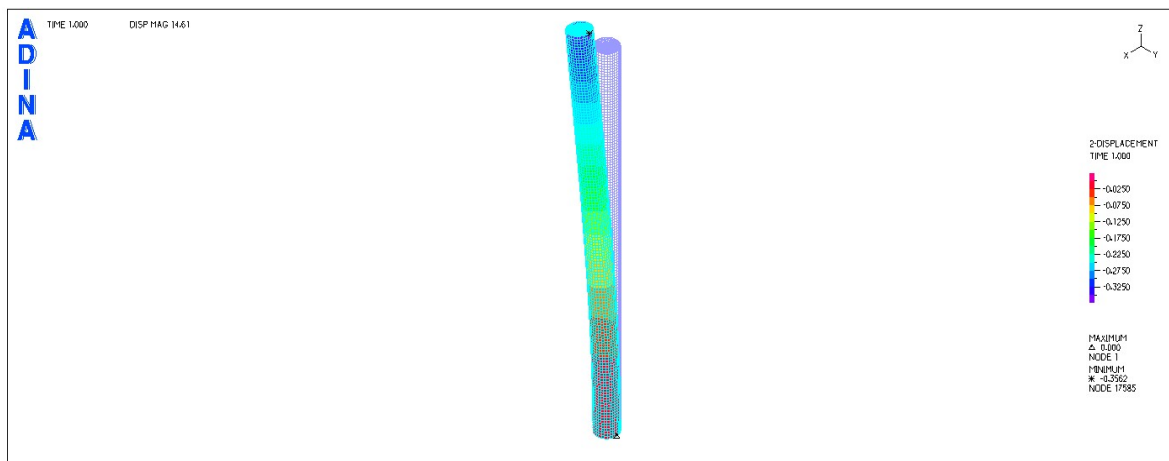

Figure 3. 16: Analysis results for the static stimulant with shell finite elements for the seismic load combination. Maximum displacement 0.36cm

Table 3. 2: New initial and reduced thickness of the chimney vertically

Part	Length (m)	Total Length (m)	Initial Thickness (mm)	Reduced Thickness (mm)	Model Internal Diameter (mm)
1	10.00	10.00	20	17	3723
2	14.00	24.00	18	15	3724
3	12.00	36.00	12	9	3726
4	22.00	58.00	10	7	3728
5	2.00	60.00	8	5	3730

3.3. Plastic limit state (LS1)

The analysis is performed according to the worst combination. The loads applied to the simulants are increased by the rates $\gamma_Q = 1.35$ and $\gamma_G = 1.50$.

In this case, the maximum von Misses stress is compared to the yield capacity of the material f_{yd}.

The von Misses maximum stress is taken straight from the software (maximum von Misses stress = 199.315 MPa) for S.S.1, while for S.S.2. it's calculated from the internal forces M, Q, N using the formulas proposed by EN1993-1-6.
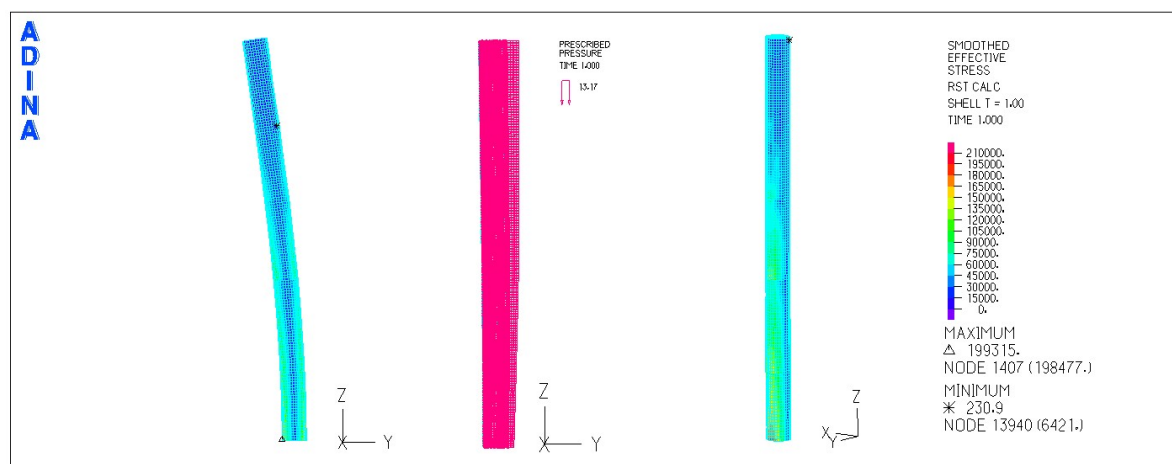

Figure 3. 17: LS1 analysis results for the static stimulant with shell finite elements

In *Table 5* the von Mises equivalent stress results and the resulting safety factors are presented. As can be seen from the results, the application of the membrane theory (through analytical formulas proposed by EN1993-1-6) underestimates the maximum von Mises stress, giving a greater safety factor. This seems to happen because, by definition, the membrane theory ignores any bending effects (which can emmerge in the base, because of the support conditions) that contribute to the stress of the body.

Also, as can be seen from
Figure 3. 17 the maximum stress occurs in the compression area of the chimney. This is because of the fact that, in the area of compression, the chimney is borne by its weight load.

Table 3.3: The von Mises equivalent stress and load ration factor using the finite element method and membrane theory.

	Numerical analysis with finite elements	Membrane theory
The von Mises equivalent stress [MPa]	199.315	173.493
Load ration factor r_{Rk}	1.731	1.989
Load ration factor r_{Rd}	1.731	1.989

The check of the LS1 can be achieved through material non-linear analysis (MNA), but also through geometry and material nonlinear analysis (GMNA). The check is performed using the plastic resistance ratio r_{Rpl} as determined in EN1993-1-6.

The loads as resulted from the worst combination (design actions taking into account the factors γ_Q and γ_G). Using the software Adina, collapse analysis is performed, initially for nonlinearity of material (MNA) and then for nonlinearity of material and geometry (GMNA). Collapse analysis is performed using the load scaling factor "λ" (Lambda). During the analysis procedure, the value of the factor gradually increases to the point of failure. Collapse analysis continues after the point of failure (branching point). It is noticeable that, in order to perform the collapse analysis, the software requires as an initial small drift somewhere in the body must be defined. The drift, obviously, is defined in the direction where the structure is expected to be deformed under the effect of specific loads (the direction is known from preliminary linear analyses).

After the end of the analysis, the equilibrium path for a given node of the model is determined (load increasing coefficient versus deformation diagram). For the chimney, a node at the top is selected to show the maximum displacement. In ***Figure 3. 18*** the four equilibrium paths, which correspond to the static analysis of two simulants, are presented (with shell and bar elements) for the MNA and GMNA analyses.

It is evident that for all four analyses the equilibrium paths are linear and almost identical for displacement up to 1.20m. Follows the branching point and then abrupt change of the slope. It is noteworthy that in S.S.2 the equilibrium path shows a sharp change in slope, with an obvious point branching. On the contrary, in the case of GMNA analysis, for the S.S.1 the equilibrium path becomes progressively nonlinear. The difference is because of the diversity of the elements used in the simulants. In S.S.1 the material yielding takes place in several discrete points of the body region, because the grid of finite elements. In contrast, in S.S.2 check of the material yielding is performed within fewer discrete points, so there is "abrupt" yielding of the material. What should be noted is that

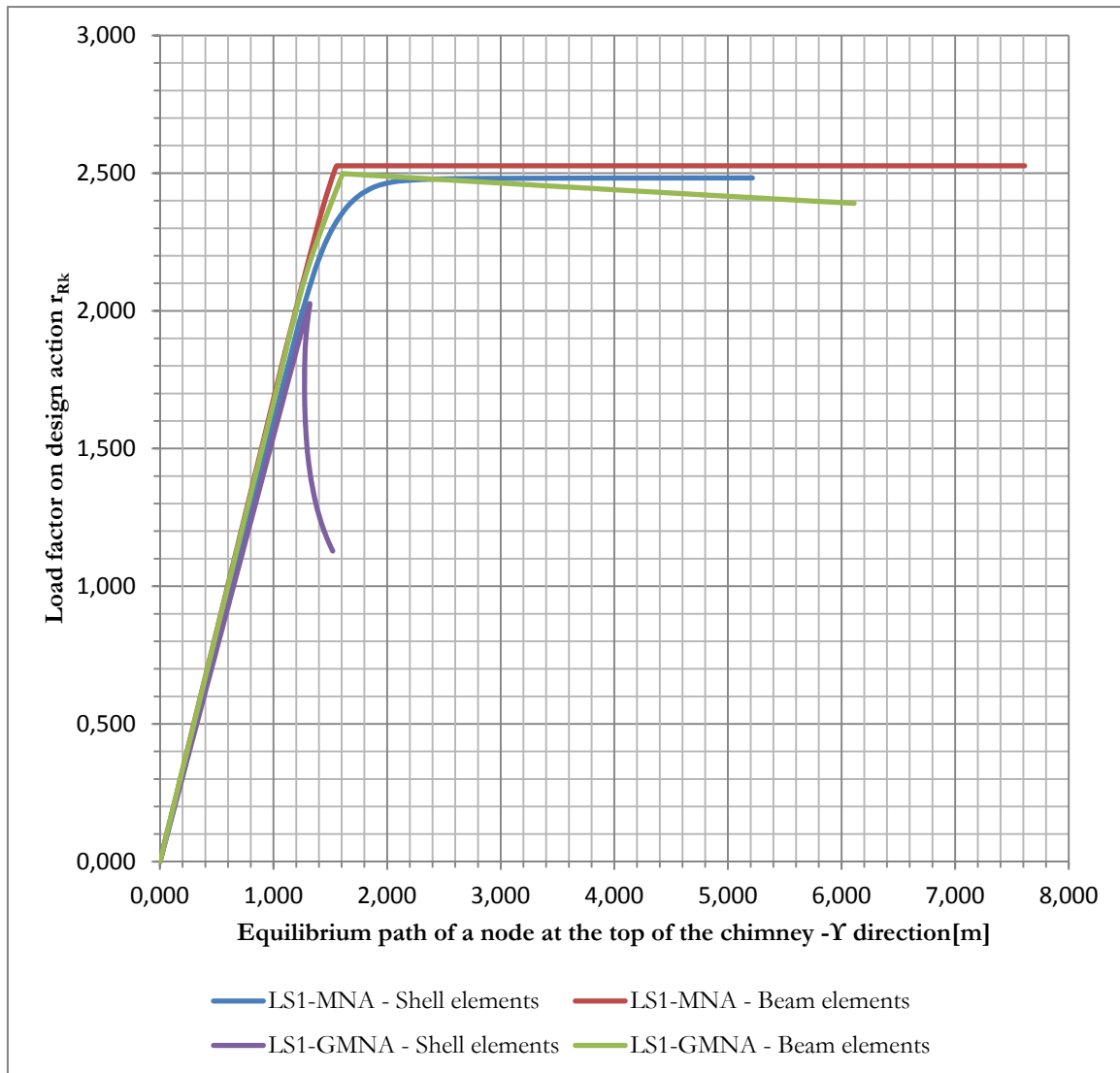the two static simulants for MNA analysis show almost the same value for the ratio of plastic resistance r_{Rk}.

Figure 3. 18: Equilibrium path of a node at the top of the chimney for MNA and GMNA analyses, for both static simulants

For GMNA analysis the equilibrium paths obtained from the two static simulants differ. In S.S.1 the equilibrium path shows before any other analysis, branching point and then follows an abrupt fall. This abrupt equilibrium path corresponds to brittle failure of the chimney due to local buckling at the base. Because of its relatively large height, any significant diversion of the chimney from the vertical axis, which is obtained through the nonlinearity in the geometry, bornes the compression zone at the base with the structure's weight. This results in encouraging the local buckling. On the contrary, in S.S.2 the equilibrium path from the GMNA analysis seems identical, to the branching point, with the corresponding equilibrium path extracted by MNA analysis. After the branching point for GMNA

analysis, the equilibrium path shows a slight decline. In S.S.2, because of the bar elements used, buckling phenomena might occur local. The fall in the equilibrium is because of the flexural buckling.

In *Table 3. 4* the values of the plastic resistance coefficients r_{Rk}, defined as the maximum value obtained from the equilibrium path for each of the analyses described above. As S.S.1 and S.S.2 are considered the static simulants with shell and bar finite elements respectively. It is easy to observe that the ratio r_{Rk} takes almost the same value for all the GMNA analyses in S.S.1, for the reasons mentioned above. The ratio r_{Rd} obtained by the function:

$$r_{Rd} = \frac{r_{Rk}}{\gamma_{M0}}$$

Where γ_{M0}=1.00

Table 3. 4: Values of the plastic resistance ratios r_{Rk} and r_{Rd} for limit state LS1, received by MNA and GMNA analyses.

	MNA		GMNA	
	S.S.1	S.S.2	S.S.1	S.S.2
r_{Rk}	2,483	2,527	2,025	2,498
r_{Rd}	2,483	2,527	2,025	2,498

Based on the EN1993-1-6, the chimney is considered to be safe versus resistant plastic limit state if applies: $r_{Rd} \geq 1$. Therefore, based on the results, the chimney is considered to satisfy the constraints for the ultimate limit state LS1 with a minimum safety factor of 2.025.

It is noteworthy that for GMNA analysis in S.S.1 and check using the analytical formulas comparable values of the safety factor are obtained. From the later derives that, for the LS1 check, the GMNA analysis is appropriate, since it simulates better the behaviour of the structure.

In *Figure 3. 19* an overview of the evolution of the deformations on the chimney using GMNA analysis is presented (at discrete points of the equilibrium path), while in *Figure 3. 20-24* is presented the stress state of the base during the change of loads. From the figures, it is easy to indicate that the failure of the chimney comes from local buckling and yielding of the material at the base.
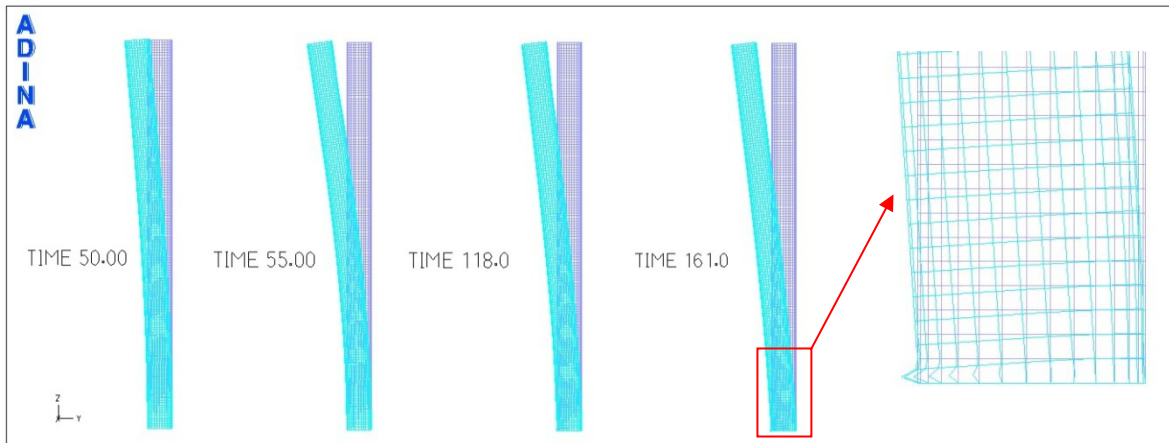
Figure 3. 19: Evolution of the deformations is specific points of the equilibrium path of the chimney, for GMNA analysis
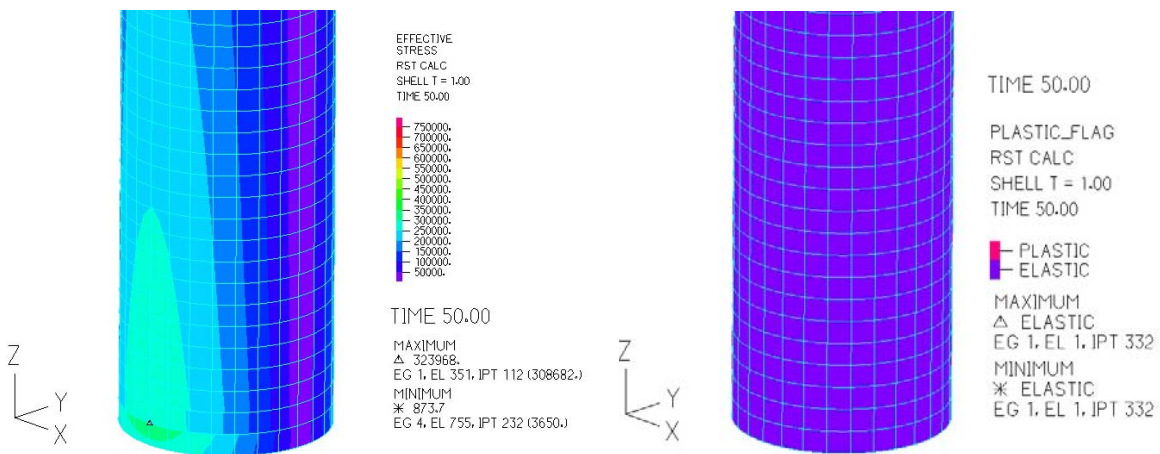

Figure 3. 20: Stress curves and deformations by GMNA analysis for load increment coefficient r_{Rk}=0.913 – pre-yielding state
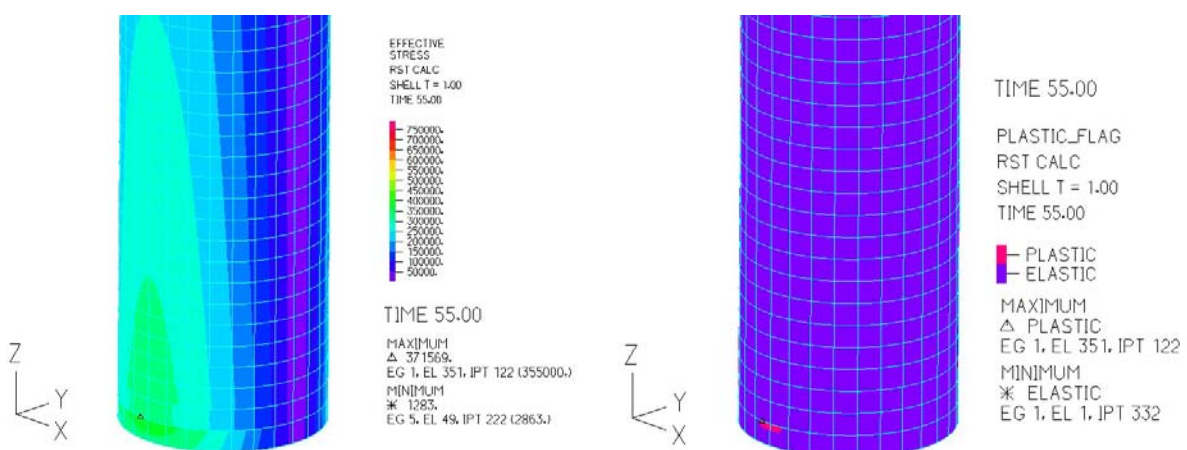

Figure 3. 21: Stress curves and deformations by GMNA analysis for load increment coefficient r_{Rk}=1.048 – post-yielding state
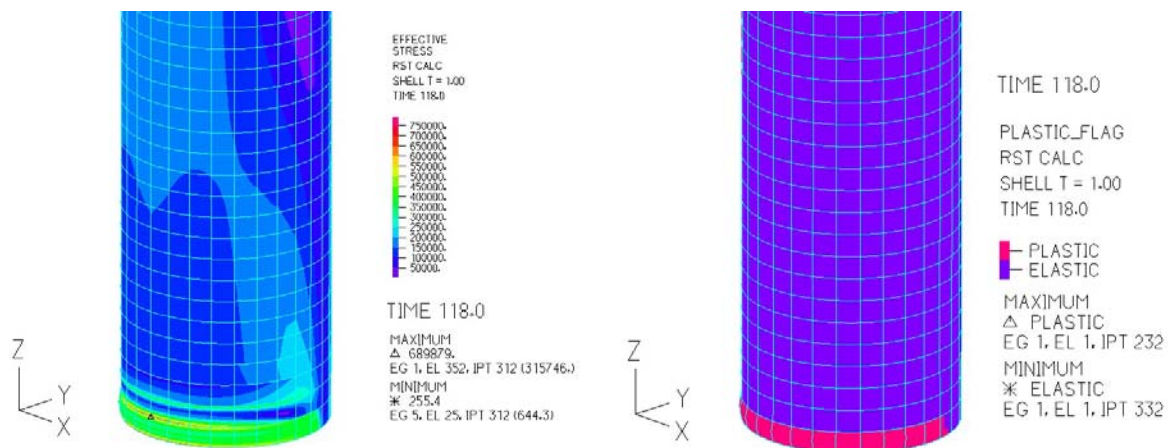
Figure 3. 22: Stress curves and deformations by GMNA analysis for load increment coefficient r_{Rk}=1.941 – before local buckling occurrence
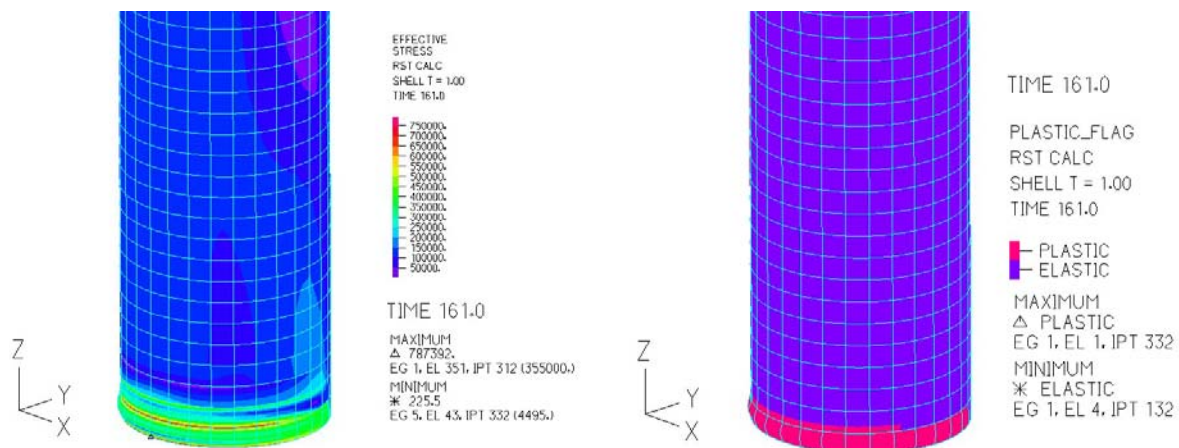

Figure 3.23: Stress curves and deformations by GMNA analysis for load increment coefficient r_{Rk}=1.128 – after local buckling occurrence (end of analysis)

3.4. Limit state of plasticity in cyclic loading (LS2)

In the LS2 analysis the typical values (γ_Q = 1.00 and γ_G = 1.00) of the actions that may be applied and removed from the structure more than three times are used.

In S.S.2 an LA analysis is performed and the values of M, Q, N are calculated. As in LS1, the values of the respective stresses are calculated using the analytical formulas of Annex A of EN1993-1-6.

From changes in the stresses, the design value of the variation of the equivalent von Misses stress is estimated according to the formula:

$$\Delta\sigma_{eq,Ed} = \sqrt{\Delta\sigma_{x,d}^2 + \sigma\Delta_{\theta,d}^2 - \Delta\sigma_{x,d}\cdot\Delta\sigma_{\theta,d} + 3\cdot\Delta\tau_{x\theta,d}^2} = 231.893 MPa$$

The resistance to equivalent range of von Misses stress variations is determined by:

$$\Delta_{feq,Rd} = 2 \cdot f_{yd} = 2 \cdot 345 MPa = 690 MPa$$

So, since:

$$\Delta \sigma_{eq.Ed} = 231.893 MPa \leq \Delta_{feq,Rd} = 690 MPa$$

The chimney is safe against plasticity in cyclic loading.

In the case of check via non-linear numerical analysis, EN1993-1-6 defines that the total accumulated von Misses stress equivalent plastic deformation should be calculated e_p, e_q, E_d at the end of the design life of the chimney. Because the operation loads are unable to cause plastic deformation, the check of limit state LS2 through numerical nonlinear analysis is not performed.

3.5. Buckling limit state (LS3)

The analysis is performed under the worst combination of loads as for LS1. The loads applied to the simulants are increased by the rates γ_Q and γ_G.

The support boundary conditions of the chimney on top and base are BC2f and BC1f respectively (according to Figure 8.1. of EN1993-1-6). However, the proposed formulas in section D1.2.1 can be applied. So, based on the stress data obtained by the LA analysis in S.S.2, the necessary checks against buckling are performed through analytical formulas defined in EN1993-1-6.

In Table 7, the results of the checks for the ultimate limit state LS3 are presented. As can be seen from the results, the testing against circumferential compression is critical. This is generally a matter to the fact that the shell of the chimney is relatively thin, so it is prone to circumferential buckling.

Thus, using the specific thicknesses of the shell, the design of the chimney against buckling takes safety factor equal to:

$$r_{Rk} = \frac{\sigma_{\theta Rd} = 0.995 MPa}{\sigma_{\theta Ed} = 0.96 MPa} = 1.036 > 1$$

which is obtained by checking against circumferential compression in the upper part of the chimney.

Table 3. 5: Check results, using stresses, for limit state LS3

Check		Συνθήκη
Check in meridian compression		$\sigma_{x,Ed} = \sigma_{eqEd} = 173.493 MPa \leq 205.043\ MPa$
Check in circumferential compression	*Upper part*	$\sigma_{\theta Ed} = 0.96 MPa < \sigma_{\theta Rd} = 0.995 MPa$
	Bottom part	$\sigma_{\theta Ed} = 0.624 MPa < \sigma_{\theta Rd} = 1.119 MPa$
Check in shear stress		$\tau_{x\theta,d} = 9.13 MPa < \tau_{Rd} = 44.723 MPa$
Interaction between shear stress, meridian and circumferential stress		$\left(\dfrac{173.493 MPa}{205.043 MPa}\right)^{1.74} + \left(\dfrac{0.624 MPa}{1.119 MPa}\right)^{1.252} + \left(\dfrac{9.13 MPa}{44.723 MPa}\right)^{1.806} = 0.941 < 1$

Then the buckling checks are performed through numerical MNA and LBA analyses. From the MNA analysis performed in paragraph 4.1 are received the values of plastic resistance ratios r_{Rk}.

For the calculation of the critical elastic buckling resistance ratio r_{Rcr} buckling modal analysis (LBA) is performed based on the calculated linear elastic state of stress of the perfect shell geometry (LA) in the design values of loads. The coefficient is taken as the smallest eigenvalue obtained (branching factor of the load). The values of the elastic buckling resistance ratio r_{Rcr}, for the first five buckling modals are presented in ***Table 3. 6***.

Table 3. 6: Values of the elastic buckling resistance ratio r_{Rcr}, for the first five buckling modals for static simulant 1.

LBA	
Buckling modal	r_{Rcr}
1	4.457
2	4.540
3	4.592
4	4.675
5	4.685

Figure 3. 25-29 show the first five buckling modals received for the static simulant with shell finite elements. Note that for purposes of LBA analysis 0.25% of the final design load was applied. Therefore, the accretion rate shown in the first five buckling modals should be multiplied by 0.25. As can be seen, all five modals correspond to local buckling phenomena at the base of the chimney. The first buckling modal corresponds to the classic case of shell buckling due to folding (cavities in the meridian). On the following modals it is obvious that cavities appear in the region.

It is understandaable that local buckling phenomena, as mentioned, cannot be observed in static simulations with fluted points (S.S.2). The ratio of the critical elastic buckling resistance r_{Rcr} for static S.S.2 take on values very large (>> 50) which, in this case was not considered realistic.

Noteworthy is the fact that ground elastic buckling resistance r_{Rcr} is a value higher than the plastic reference resistance ratio r_{Rpl}. This is because the chimney is not is stressed by significant axial loads and so it seems that the structural material yields before the local buckling occurs.

Thus, from the results, the ratio of the characteristic buckling resistance r_{Rk} is calculated as:

$$r_{Rk} = \chi_{ov} \cdot r_{Rpl}$$

where χ_{ov} is the buckling reduction factor, which is calculated as $\chi_{ov} = f\left(\overline{\lambda}_{ov}, \overline{\lambda}_{ov,0}, a_{ov}, \beta_{ov}, \eta_{ov}\right)$

The total normalized slenderness λ_{ov} of the shell is calculated by:

$$\overline{\lambda}_{ov} = \sqrt{\frac{F_{R_{pl}}}{F_{R_{cr}}}} = \sqrt{\frac{r_{R_{pl}}}{r_{R_{cr}}}} = 0.746$$

Values of $\lambda_{ov}, \lambda_0, \beta_{ov}, \eta_{ov}$ και r_{Rov} are calculated conservatively in Section D.1.2.2 as:

$$\overline{\lambda}_{ov,0} = \overline{\lambda}_{x0} = 0.20$$
$$\beta_{ov} = \beta = 0.60$$
$$\eta_{ov} = \eta = 1.0$$

The total defects reduction factor α_{ov} is calculated from the formula:

$$a_{ov} = \frac{0.62}{1 + 1.91\left(\dfrac{w_k}{t}\right)^{1.44}}$$

From previous reports:

$$a_{ov} = 0.304$$

So the value of the plastic normalized slenderness limit is:

$$\overline{\lambda}_p = \sqrt{\frac{a}{1-\beta}} = 0.871$$

Therefore, because $\overline{\lambda}_{ov,0} \leq \overline{\lambda}_{ov} \leq \overline{\lambda}_p$

$$\chi = 1 - \beta \left(\frac{\overline{\lambda}_{ov} - \overline{\lambda}_{ov,0}}{\overline{\lambda}_p - \overline{\lambda}_{ov,0}} \right)^{\eta} = 0.512$$

So the ratio of safety factor r_{Rk} is:

$$r_{Rk} = 0.512 \cdot 2.483 = 1.271$$

Thus the ratio of the characteristic buckling resistance r_{Rk} is:

$$r_{Rd} = 1.271 / 1.1 = 1.155 > 1$$

Because the coefficient r_{Rd} takes a value greater than one, the chimney is considered to be safe against buckling.

As can be seen, the check of the ultimate limit state through LS3 using MNA analysis gives greater safety factor than the previous corresponding calculations through streses. This happens because in the MNA analysis, the material nonlinearity is also taken into account.
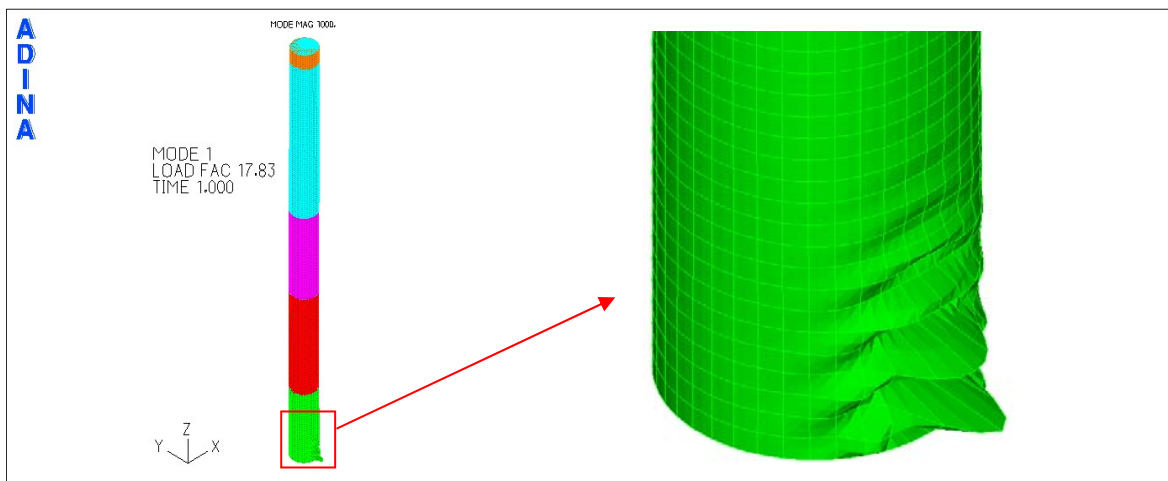

Figure 3. 24: 1st buckling modal of the static stimulant with shell finite elements – LBA analysis.
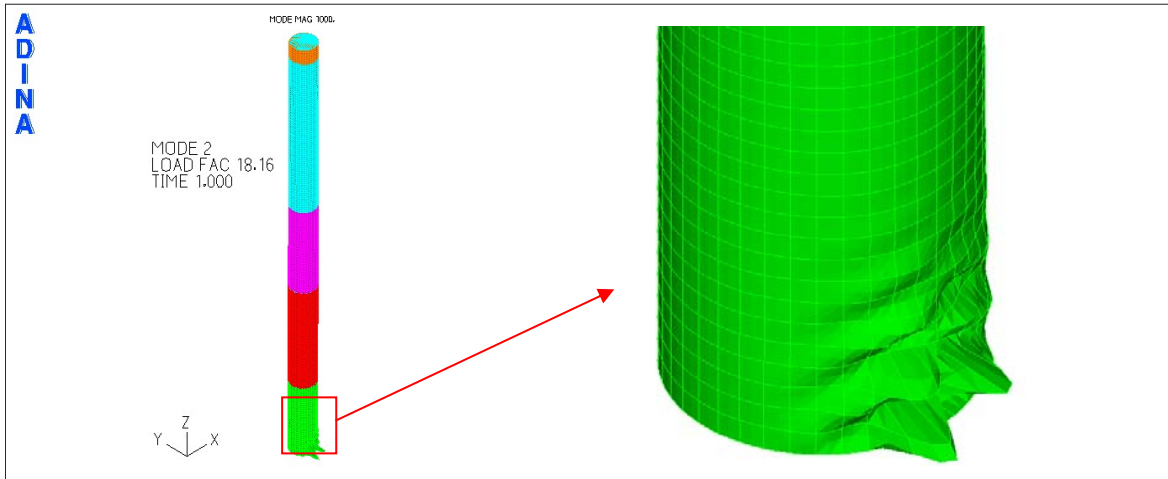
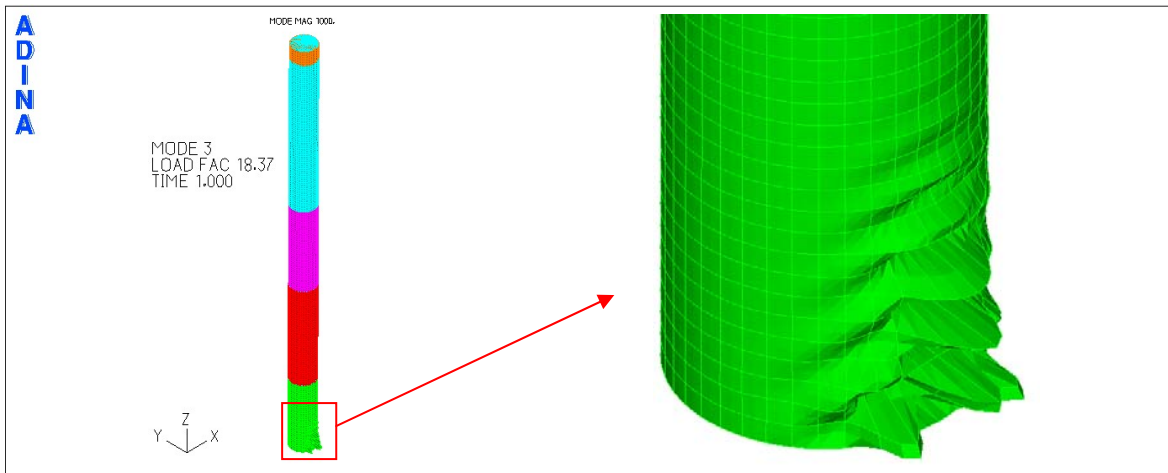**Figure 3. 25:** 2nd buckling modal of the static stimulant with shell finite elements – LBA analysis.

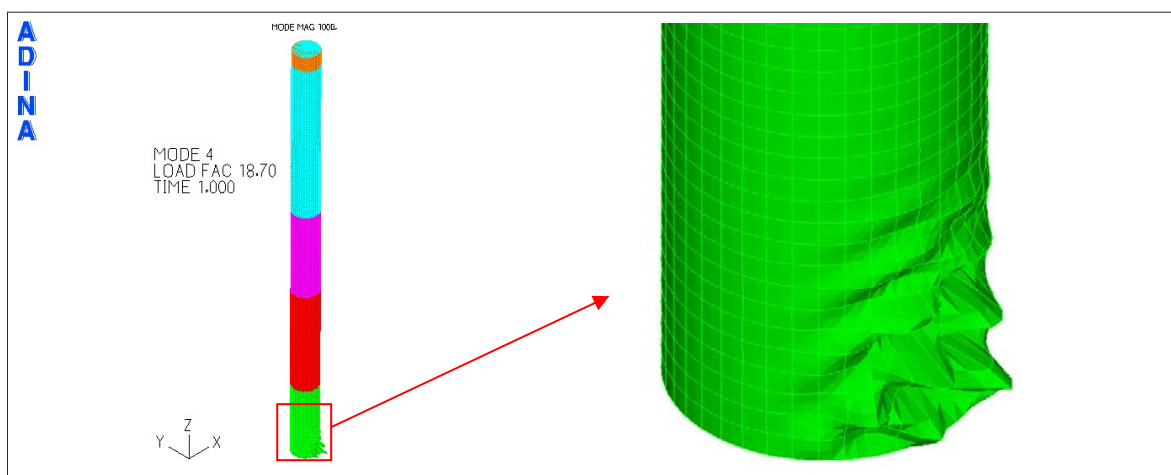**Figure 3. 26:** 3rd buckling modal of the static stimulant with shell finite elements – LBA analysis.

Figure 3. 27: 4th buckling modal of the static stimulant with shell finite elements – LBA analysis.
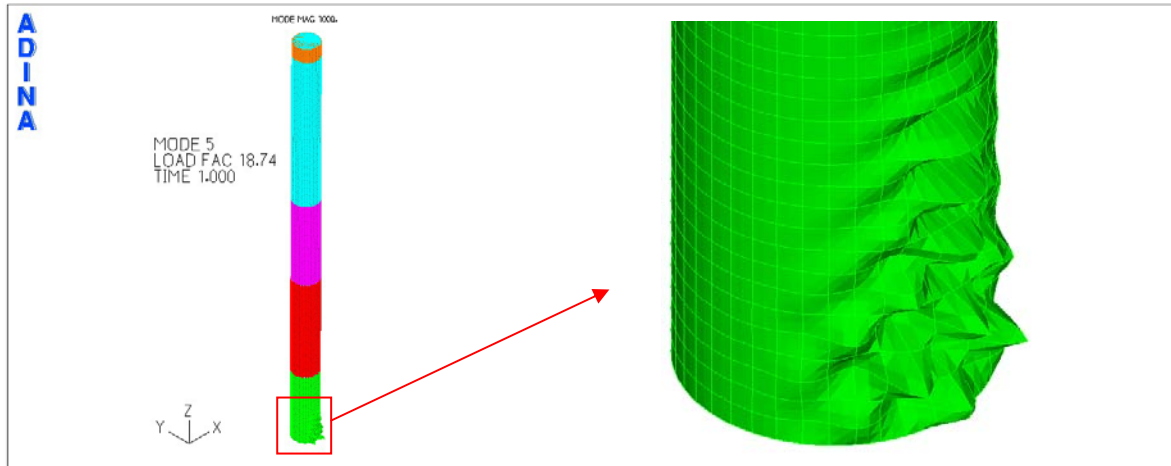
Figure 3. 28: 5th buckling modal of the static stimulant with shell finite elements – LBA analysis.

The check against buckling can be also achieved through non-linear numerical analysis that takes into account the nonlinearity of material and geometry, as well as potential flaws in the structure's shell (GMNIA). EN1993-1-6 defines three types of defects that could appear in a shell body and should be considered in the analysis. Defects regarding a possible deviation from the circular shape, random eccentricity and due to folding.

For the purposes of this study, only possible defects due to body folding are taken into account. The defects are considered in the analysis by the buckling modal and are defined by the relevant displacements of the nodes of the model for the first modal buckling. For this specific example, the first five buckling modals are taken into account. For each modal is detected the node of the grid of finite elements with the maximum displacement and there is defined the maximum displacement due to defects. The displacements of the other nodes are proportional to the maximum specified displacement.

For the shell of the chimney an offset from the circular shape is considered equal to $U_{r,max} = 0.016$. This value corresponds to the maximum value of the tolerance parameter for the crimp of the shell. So, the maximum allowed defect of the shell due to folding is calculated as follows:

$$l_{gx} = 4 \cdot \sqrt{r \cdot t} = 4 \cdot \sqrt{r \cdot t} = 1.01m$$

$$U_{0,i} = \frac{\Delta w_{0i}}{l_{gi}} \Rightarrow \Delta w_{0x} = U_{0,x} \cdot l_{gx} = U_{r\max} \cdot l_{gx} = 0.016 \cdot 1.01m = 16.16mm$$

Following, a non-linear analysis of geometry and material, including defects (GMNIA). From this analysis the equilibrium path of a node at the top of the chimney which is shown in **Σφάλμα! Το**

αρχείο προέλευσης της αναφοράς δεν βρέθηκε.. is extracted. In the same figure, for comparison purposes, is given the equilibrium path obtained through
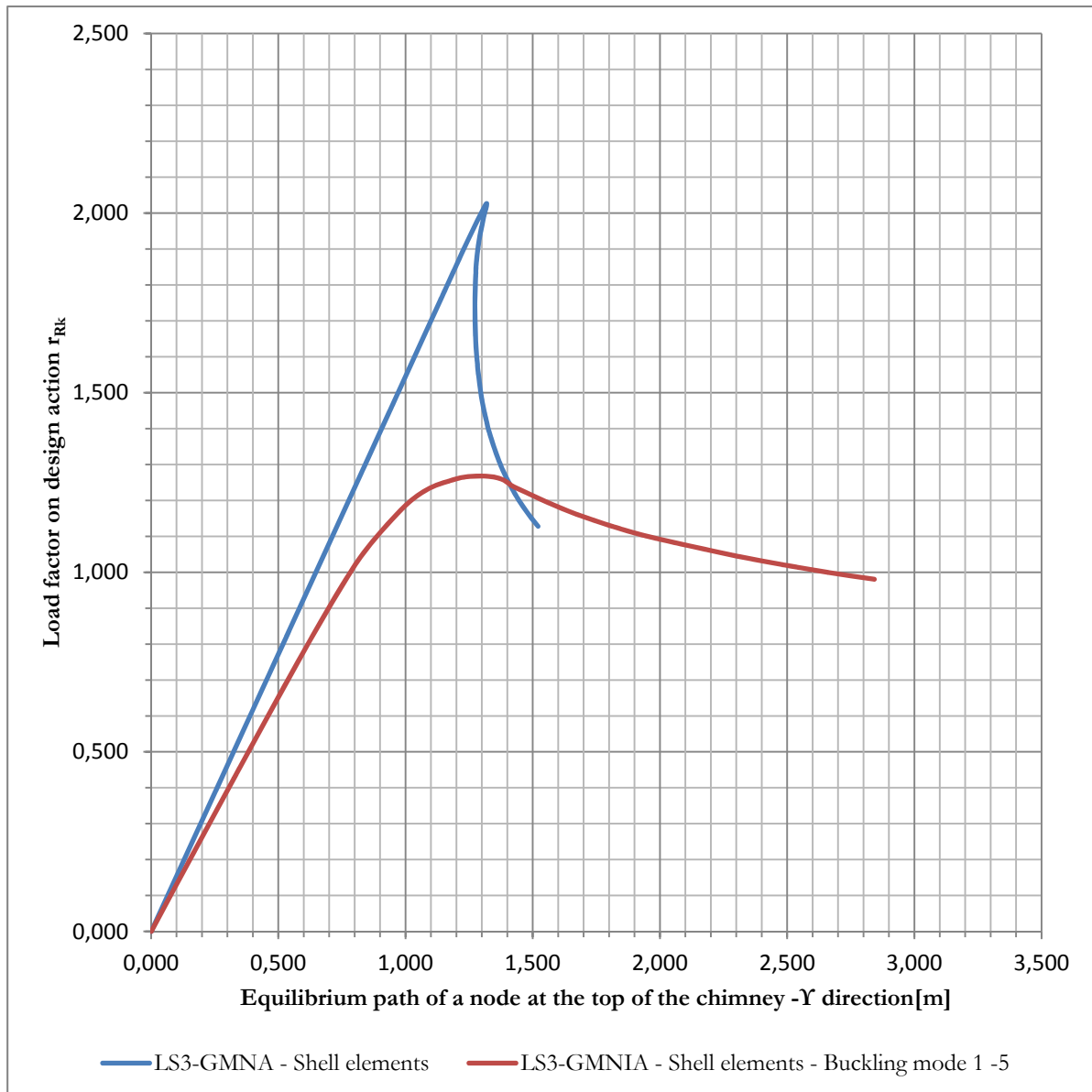

Figure 3. 29: Equilibrium path of a node at the top of the chimney - GMNA and GMNIA analyses

GMNA analysis. As can be seen, the two equilibrium paths differ greatly and this verifies the influence of defects on the stability of the structure. The influence of defects is evident from the beginning of the   chimney's deformation. From the equilibrium position until 0.80 m peak deformation, the equilibrium path remains linear but with less pitch from that obtained from the equilibrium path of the peak under GMNA analysis. For only 1.30m peak displacement, the chimney

develops the highest resistance for GMNIA analysis. Immediately after this point, failure due to local buckling occurs at the base, so the path follows a downward direction. Then, the equilibrium path tends to become horizontal. For reasons of computational "cost", the analysis was interrupted for peak deformation equal to 3m. For supervisory purposes, in **Figure 3. 30** and *32* are presented respectively the deformation and stress on the base of the chimney, after the end of the analysis.

From the GMNIA analysis the ratio of endless elasto-plastic buckling resistance r_{RGMNIA} is received as the maximum value derived from the equilibrium path (see Figure 7.9). Thus:

$$r_{RGMNIA} = 1.268$$

EN1993-1-6 defines that there should be check for the reliability of the figures identified numerically defined endless elasto-plastic buckling resistance ratio r_{RGMNIA}. From checks, the calibration coefficient k_{GMNIA} is extracted. The calculated value of the ratio should not exceed 1.0. Also, the coefficient should not take values beyond:

$$0.8 \leq k_{GMNIA} \leq 1.2$$

For the purposes of this study, the calibration coefficient is taken conservatively equal to:

$k_{GMNIA} = 0.9$

Thus the ratio of the ratio of the characteristic buckling resistance is:

$$r_{Rk} = k_{GMNIA} \cdot r_{R,GMNIA} = 0.9 \cdot 1.268 = 1.141$$

And so the design resistance ratio to buckling r_{Rd} is:

$$r_{Rd} = 1.141 / 1.1 = 1.037 > 1$$
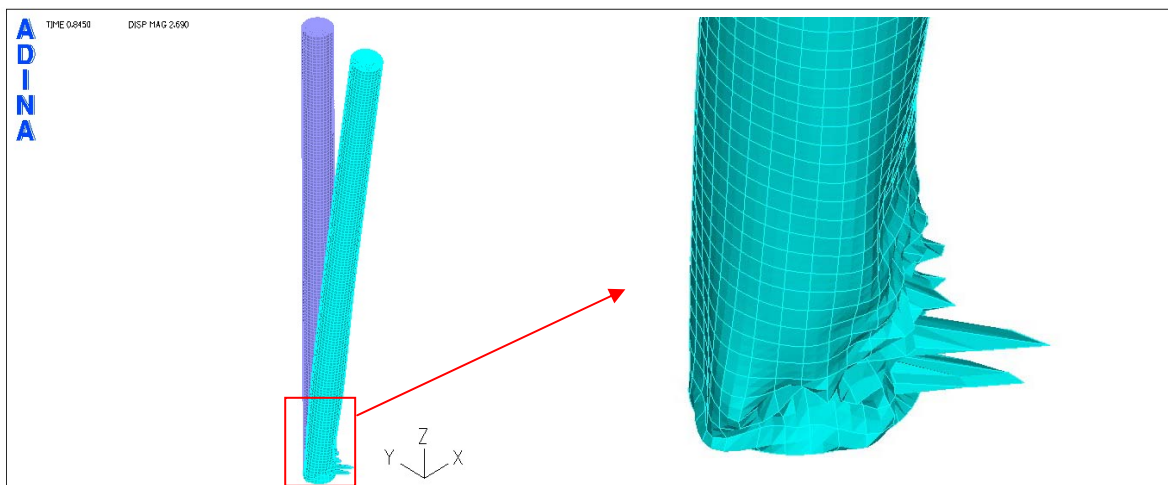
So the chimney is safe against buckling.

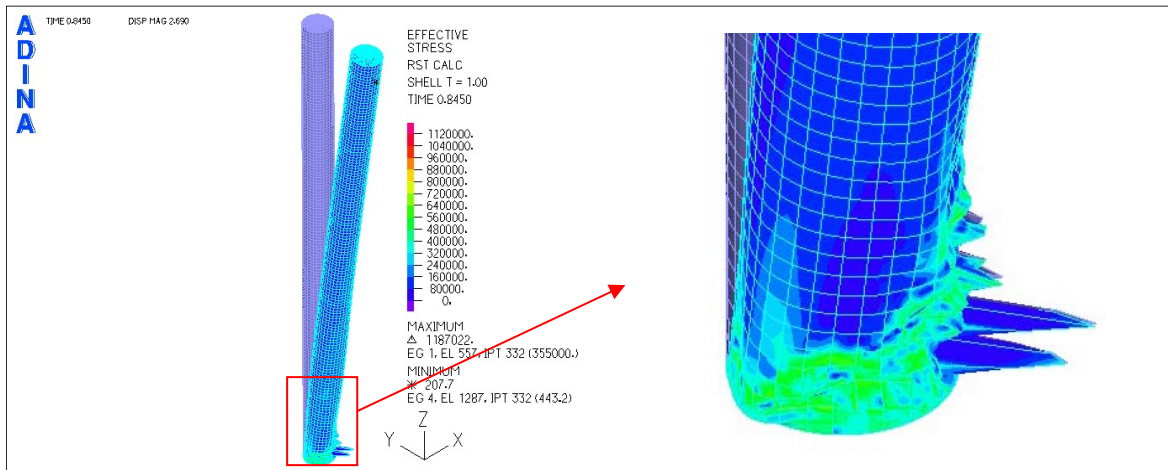***Figure 3. 30:*** Deformation of the chimney by GMNIA analysis

Figure 3. 31: Maximum stresses in the chimney by GMNIA analysis

It is evident from the results, that from GMNIA analysis lower safety factor is received, than from GMNA analysis. Defects in the shell apparently play an important role in the stability of the chimney.

The choice of the most relevant defects, which will result in lower safety factor, is a major matter for a GMNIA analysis. EN1991-1-6 provides that the choice of defects should be performed after a test procedure.

For purposes of this work, parametric analysis is performed for the selection of an adequate number buckling modals. Regarding the latter, it should be noted that the number of modals, which will be taken into account in the analysis, is not always depending on the disfavour of the results. It is very likely, in case of combination of buckling modals, that the deformations will cancel each other, due to sign difference. For this reason, it was considered appropriate to investigate whether in this case is appropriate to take a number of buckling modals or should each one individually.

In **Figure 3. 32** the equilibrium paths of a node at the top of the chimney for GMNIA analysis are presented. For the chimney two extra different GMNIA analyses were performed considering separately the first and second buckling modal.

As can be seen, in this case the combination of the first five buckling modals seems to result in the smallest buckling safety factor. Unlike, when the GMNIA analysis was performed for individually the first and second buckling modals, the safety factor seems to have received higher values.
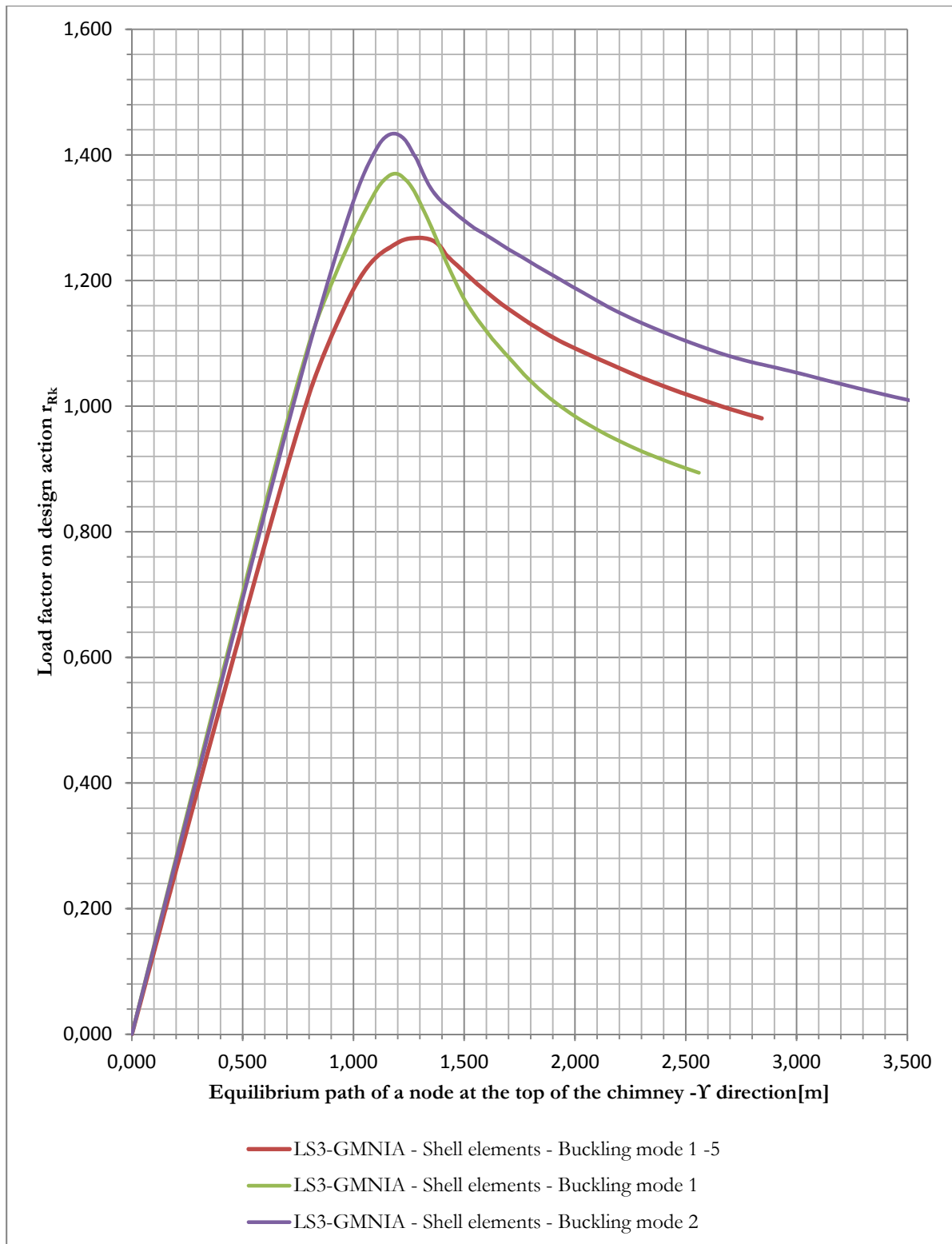
Figure 3. 32: Equilibrium path of a node at the top of the chimney received by GMNIA analysis for a different number of buckling modals

3.6. Fatigue (LS4)

As set out in Section 3, the chimney should be evaluated against turbulent excitation. Based on the calculations, the range of vibration calculated for the chimney, under the influence of turbulent excitation, is 2.69m. According to EN1993-3.2, this range is prohibitive. For this reason, measures to reduce the range of vibration should be taken. For the reduction of the range of vibration, aerodynamic devices and / or dampers can be used. If aerodynamic devices are used, the maximum range of vibration should be calculates in accordance with the method 1. However, as described in Section 3, this method underestimates the range of vibration. So, in the example the results emerged from the second method are used. For this reason, in order to reduce the transverse vibration range, tuned mass damper is placed on the chimney (TMD).

But, for purposes of this study and for comparison reasons, the reduction of the transverse vibration range using aerodynamic equipment is estimated. So, if the method 1 (for the calculation of the maximum vibration range) gave realistic results, then by the formula:

$$a = \left(1 - \frac{P_s}{h}\right)^3$$

and under the assumption that spiral spoiler will be mounted on the 1/3 of the top height of the chimney, then:

$$a = \left(1 - \frac{20}{60}\right)^3 = 0.30$$

and therefore the aerodynamic device would provide a reduction in the maximum range of vibration equal to 70%. Therefore, the final range of vibration, based method 1, would be:

$$y_{Fj} = 0.269 \cdot 0.3 \cdot b = 0.301m$$

So, assuming that the chimney is of reliability class 2, then the maximum range of vibration due to turbulent agitation should not be larger than 0.10xb = 0.37m. Therefore the maximum range of vibration satisfies the restrictions.

Finally, however, it is considered that damper will be placed in the chimney, which will add to the chimney damping equal to δs = 0.3. Therefore the Structon number becomes:

$$Sc = \frac{2 \cdot \delta_s \cdot m_{i,e}}{\rho \cdot b^2} = 39.105$$

and

$$\frac{y_{F,\max}}{b} = 0.014$$

therefore, the maximum range of vibration, according to method 2 of EN1991-1-4, is:

$$y_{F,\max} = 0.051m < 0.37m$$

Based on this range, the inertial force, due to turbulent agitation, is calculated in accordance with Annex E of EN1991-1-4.

The loads are applied to two static simulants. The check for fatigue takes place at the base of the chimney in accordance with EN1993-1-9. For the chimney a lifetime of T = 25 years is used. The chimney is welded at its base on a frontal plate with a 40mm thick front-butt T welding.

According to the case (20) in Table C.1 of EN1993-3-2, the weld should be checked at two points, i.e. at the upper point of the weld which in contact with the shell of the chimney (20mm thick) and bottom point, which is in contact with the frontal plate.

Design against fatigue using stresses (LA) or numerical analysis (GNA) is considering the variation of the stresses due to turbulent stimulation. EN1993-1-6 does not provide any specific instructions regarding the LA or GNA analysis.

The calculation of the design stress at the base of the chimney is performed by calculating the design moment for S.S.2 and calculation of average stress design by S.S.1. In ***Table 3. 7*** are presented the values of the above mentioned, as received from the two static simulants.

Table 3. 7: Stress magnitudes used in the check against fatigue for the two simulants.

	Simulant 1	Simulant 2
$\Delta\sigma_c$[MPa]	33.076	---
M_{sd}[kNm]	---	2138

Since the wind direction is random, variation in stresses for simulant 2 is taken as twice the maximum stress developed in one wind direction:

$$\Delta\sigma_s = \frac{2 \cdot Msd}{w} = \frac{2 \cdot Msd}{\pi \cdot r^2 \cdot t} = 30.652 MPa$$

The number of cycles of vibration due to turbulent agitation (N) is calculated, and from the curves of fatigue capacity (EN1993-1-6) the coefficient k is received equal to:

$$\lambda = \lambda_1 \cdot \lambda_2 = 2.672$$

The check against fatigue is performed at the top and bottom of the weld

• Check of the upper point of the base welding

For high-quality performance welding at both sides of the plate, the matter of detail are:

$$\Delta\sigma_c = 125MPa$$

The determination of safety against fatigue due to turbulent excitation is as follows:

$$\gamma_{Ff} \cdot \lambda \cdot \Delta\sigma_s = 1.20 \cdot 2.672 \cdot 33.076MPa = 106.055MPa \leq \frac{125MPa}{1.15} = 108.696MPa$$

So the criterion is satisfied.

• Check of the bottom point of the base welding

The bottom point of the welding is designed in accordance with the detail (11.2) of Table C.1. So, for continuous transverse welding of the shell to the base plate and welding quality 5, the category of detail is:

$$\Delta\sigma_c = 90MPa$$

The variation of acting stresses is:

$$\Delta\sigma_s = 30.652 \cdot \frac{20}{40} = 16.538MPa$$

Thus, the determination of safety against fatigue due to turbulent excitation is as follows:

$$\gamma_{Ff} \cdot \lambda \cdot \Delta\sigma_s = 1.20 \cdot 2.672 \cdot 16.538MPa = 53.027MPa \leq \frac{90MPa}{1.15} = 78.261MPa$$

So the criterion is satisfied.

As can be seen, the check against fatigue of the connections plays an important role in the design of the chimney. From the calculations, can be determined that the welding at the base of the chimney meets the security checks at the rate of only 1.024 (upper welding point check). In order to increase the rate of disuse the weld thickness of the shell at the base with the front plate should be increased.

3.7. Serviceability limit state check

The limit value of deformation in the direction of the wind at the top of a self-standing chimney, due to the frequent repetition of the wind load, is estimated by:

$$\delta_{max} = \frac{h}{50}$$

where h is the height of the chimney.

The regular value of the wind results from the design value multiplied by the design factor $\psi_1 = 0.6$. So, the load combination for the serviceability limit state is:

$$1.00G + 0.6W$$

The values of the top displacement of the chimney for the load combination above, for both static simulants, are shown in **Table 10**. Respectively, in **Figures 34 and 35** the deformation of the chimney is presented in magnification.

Table 3. 8: Top displacements of the chimney, based on the load combination for serviceability limit state.

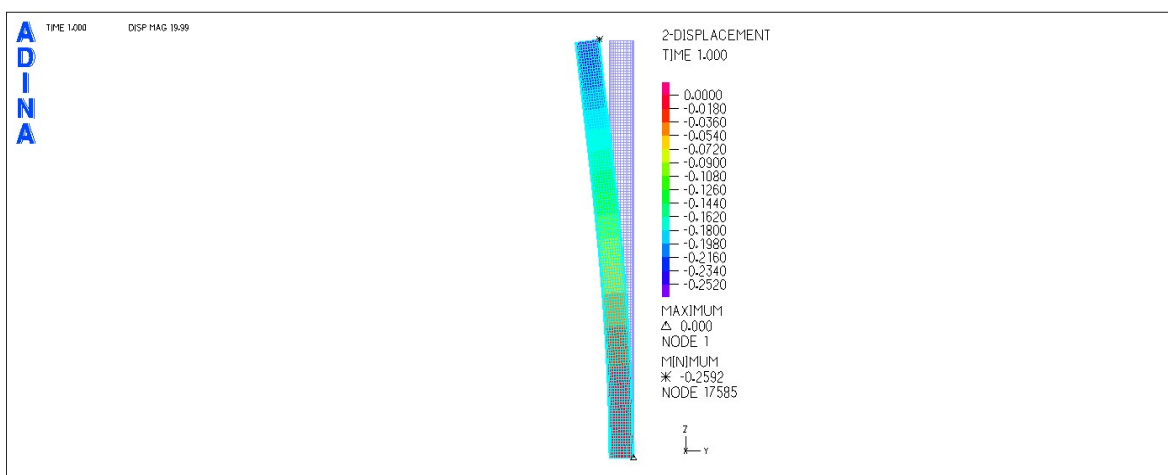|	Absolute value of the chimney's top displacement [m]
S.S.1	0.259
S.S.2	0.258

Figure 3. 33: Chimney's deformation for the frequent magnitude of the wind pressure for S.S.1
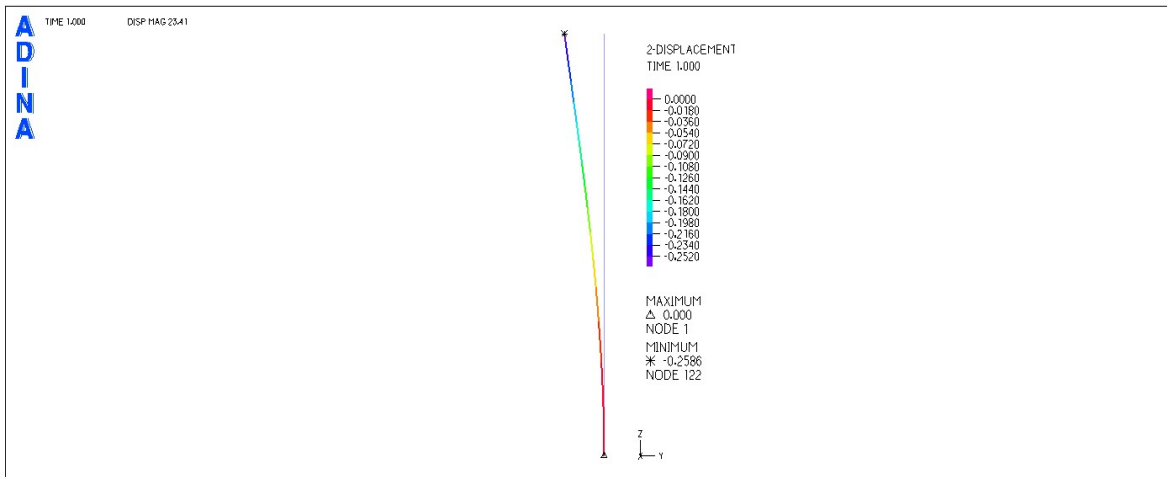
Figure 3. 34: Chimney's deformation for the frequent magnitude of the wind pressure for S.S.2

The maximum allowed deformation in the direction of the wind is:

$$\delta_{max} = \frac{60m}{50} = 1.20m$$

Obviously:

$$\delta = 0.259m < \delta_{max} = 1.20m$$

so the travelled distances due to wind load is within the limits.

4
CONCLUSIONS

In the present thesis was studied the simulation and design process of a steel chimney with diameter 3.735m and height 60m.

As proved in this example, the stability of the chimney appears to be more affected by wind loads rather than the seismic loads. Because of its dimensions, the chimney seemed to be affected more by the periodic diffusion of the vortexes due to wind flow. The maximum range of vibration due to turbulent excitation calculated did not satisfy the constraints of EN1993-3.2. So, the chimney was supposed to be equipped with a tuned mass damper at the top, which will provides damping $\delta s = 0.3$. After consideration of the additional damping, due to damper, the maximum range of vibration, due to turbulent agitation, decreased dramatically.

From the limit state checks set by EN1993-1-6, was shown that the formulas proposed in the same article give the smallest safety factor for the respective checks by nonlinear analyses.

From the non-linear analyses performed, was shown that the GMNIA analysis gives the smallest safety factor for design against ultimate limit state. Through GMNIA analysis can be simulated possible defects in the shell of the chimney. As shown, possible defects in the shell play a key role in the stability of the chimney. Both the behaviour and the safety factors resulting from GMNIA and

GMNA analyses differ. This verifies the influence of defects on the resistance and behaviour of steel chimneys.

Finally, it appeared that for the check of the chimney, the static stimulant with bar finite elements is not considered to be appropriate. Because the elements used, defects on the shell of the chimney cannot be taken into account. It is also not possible in the analysis to occur failures due to local buckling in the shell of the chimney. So, it's not advisable to use static stimulant with bar elements for modelling chimneys, since it seemed to overestimate the safety coefficient against limit state failure.

5
REFERENCES

[1] CICIND, *Model Code for Steel Chimneys*, Revision 1 – December 1999

[2] Dyrbye, C., Hansen, S.O. *Wind Loads on Structures*. Wiley, New York, 1996.

[3] EN 1993-1-6 Eurocode 3: Part 3.2, Towers, masts and chimney -Chimneys.

[4] EN 1993-1-6 Eurocode 3: Part 1.9, Fatigue.

[5] EN 1991-1-4 Eurocode 3: Wind loads

[6] Manohar S N. *Tall chimneys – Design and Construction*. Tata McGraw-Will publishing company ltd, India, 1985.

[7] International committee on industrial chimneys. *Chimney Book – Industrial Chimneys of concrete or steel*. CICIND, Zurich, Switzerland, 2005.

[8] Ishizaki H, Hara H, Shimada T. *The efficiency of helical strakes for suppression of vortex-excited vibration of steel stacks,* Journal of Structural Engineering, 1984 Vol.6, October.

[9] Zdravkovich, M.M, Kawecki J. *Cross-wind vibration of steel chimney – A new case history,* Journal of Wind Engineering and Industrial Aerodynamics, 95 (2007) 1166-1175.